Studies on the Apg12-Apg5・Apg16 complex essential for autophagy

Akiko Kuma

DOCTOR OF PHILOSOPHY
Department of Molecular Biomechanics
School of Life Science
The Graduate School of Advanced Studies

2002 (School Year)

Acknowledgements

I wish to express deepest appreciation to Prof. Yoshinori Ohsumi for his constant supervision and fruitful advices throughout this study. I would also like to express my gratitude to Dr. Noboru Mizushima for his extensive advices and insightful discussions on my study. I am grateful to Mr. Yoshinori Kobayashi for his contribution in this work. He discovered and isolated Apg16L. And I wish to thank Dr. Toshifumi Takao, Dr. Masami Matsubae and Dr. Tohru Natsume for their splendid mass spectrometric analysis. I am grateful to Dr. Naotada Ishihara for his technical assistance and for providing antibodies, Dr. Takayoshi Kirisako for providing *apg* disruptants, and Dr. Yasuyoshi Sakai for providing the amino acid sequence of *Pichia pastoris Paz3* before publication. I also express my thanks to my labmates, Dr. Takeshi Noda, Dr. Yoshiaki Kamada, Dr. Kuninori Suzuki, Dr. Yoshionobu Ichimura, Dr. Takayuki Sekito, Dr. Kohki Yoshimoto, Dr. Takao Hanada, and Ms. Yukiko Kabeya, Maho Hamasaki, Masami Miwa, Kumi Tsukeshiba, Yoko Hara and Mr. Jun Onodera for their continuous support and good company along my stay in National Institute for Basic Biology. Finally, I wish to express to my deepest thanks to my parents for their physical and spiritual support.

January 10, 2003

Akiko Kuma

Contents

Abbreviations

ALP	alkaline phosphatase
API	aminopeptidase I
CFP	cyan fluorescent protein
Cvt	cytoplasm to vacuole targeting
EDTA	ethypenediamine tetraacetic acid
ES	embryonic stem
FCS	fetal calf serum
FKBP	FK506-binding protein
GFP	green fluorescent protein
GST	glutathione *S*-transferase
HA	hemagglutinin
HEPES	*N*-2-hydroxyethylpiperazine-*N*'-2-ethanesulfonic acid
IPTG	isopropylthio-b-D-galactopyranoside
ORF	open reading frame
PAS	pre-autophagosomal structure
PAGE	polyacrylamide gel electrophoresis
PBS	phosphate-buffered saline
PE	phosphatidylethanolamine
PIPES	1,4-piperazinediethanesulfonic acid
PMSF	phenylmethlsulfonylfluoride
RT-PCR	reverse transcribed PCR
SD	synthetic dextrose medium
SDS	sodium dodecyl sulfate
TCA	trichloroacetic acid
YFP	yellow fluorescent protein

Summary

In eukaryotic cells, the majority of intracellular bulk degradation occurs in the vacuole/lysosome, an acidic compartment that contains various hydrolytic enzymes. Autophagy is the main pathway to deliver cytoplasmic components to the vacuole in yeast, or to the lysosome in mammalian cells, for degradation. In this process, portion of cytoplasm are sequestered within the double-membrane structure termed autophagosome, which subsequently fuses with the vacuole/lysosome. The sequestered components are, then, degraded by the vacuolar or lysosomal hydrolases for reuse. The best-known role of autophagy is a cellular survival response to starvation, but it also plays important roles in developmental process and cell differentiation.

Taking advantage of yeast genetics, autophagy defective mutants (*apg*) were isolated and so far 15 *APG* genes have been cloned. All of them seem to be involved in the step of autophagosome formation. During the characterization of Apg proteins, a ubiquitin-like conjugation system, the Apg12 system, was found to be essential for autophagy. In this system, Apg12 is covalently bound to Apg5, which is catalyzed by Apg7 and Apg10. Mammalian homologues of Apg12 and Apg5 have been identified and undergo a similar covalent linkage, indicating that this conjugation system is conserved in mammalian cells. Studies using mammalian cells further revealed that the Apg12-Apg5 conjugate localized to pre-autopagosomal membrane and is required for elongation of the membrane to form a complete spherical autophagosome. But the exact molecular role of the Apg12-Apg5 conjugate is still unknown.

Recently, Apg16 was found to interact with the Apg12-Apg5 conjugate in yeast. Apg16 is a 150-amino acid protein that contains a carboxyl-terminal coiled-coil motif. Since Apg16 is the only molecule identified to interact with the Apg12-Apg5 conjugate and required for function of the conjugate, further characterization of Apg16 would provide valuable insights into the molecular role of the Apg12-Apg5 conjugate. In this study, I found that Apg12-Apg5 conjugate formed a ~350-kDa complex with Apg16 in the cytosol of yeast cells, irrespective of autophagy induction. As Apg16 formed homo-oligomer through the coiled-coil region and

cross-linked Apg12-Apg5, I generated an *in vivo* system that allows us to control the oligomerization state of Apg16. With this system, I demonstrated concretely that formation of the ~350-kDa complex depends on oligomerization of Apg16 and formation of this complex is required for autophagy in yeast.

Although the Apg12-Apg5 conjugation system is highly conserved among eukaryotes, there is no significant homologue of Apg16. In mammalian cells, the Apg12-Apg5 conjugate forms a ~800-kDa complex, much larger than the yeast Apg12-Apg5·Apg16 complex. Purification of this ~800-kDa complex identified a novel Apg5-interacting protein containing seven WD repeats. I demonstrated that this newly WD repeat protein, named Apg16L, is a functional counterpart of yeast Apg16. Mouse Apg16L interacts with Apg5 at its amino-terminal region and forms a homo-oligomer through its coiled-coil region to form the ~800-kDa complex as yeast Apg16. Apg16L associates with pre-autophagosomal membrane with the Apg12-Apg5 conjugate, suggesting that the ~800-kDa complex functions in autophagosome formations in mammalian cells.

Since multiple homologues of Apg16L exist in higher eukaryotes, the autophagic machinery is well conserved through evolution. On the other hand, WD domain, which is thought to be a platform for protein-protein interaction, is not found in yeast Apg16. As the WD domain of Apg16L is not required for interaction with Apg5 and homo-oligomerization, the ~800-kDa complex is expected to interact with other proteins. Identification of such proteins would be helpful to understand the molecular mechanism of the Apg12-Apg5 conjugate in autophagosome formation.

Introduction

I. Protein degradation in eukaryotic cells.

Intracellular protein degradation plays essential roles in a number of cellular processes. It is involved in elimination of abnormal and denatured proteins, modulation of metabolic pathways by removal enzymes and post-translational processing to activate enzymes. In addition, it serves an important source of amino acids for biosynthetic reactions, especially when exogenous nutrients are not available. Eukaryotic cells have two major avenues for the degradation of proteins and organelles, the proteasome and lysosome/ vacuole systems. The proteasome is a compartmentalized proteases with multiple catalytic sites, whereas the lysosome is the major degradative organelle. In general, the proteasome participates in the selective degradation of ubiquitinated proteins, while the lysosome is involved in bulk degradation.

The ubiquitin system

The selective degradation of proteins is carried out by the ubiquitin-proteasome system (Hochstrasser, 1996; Hershko and Ciechanover, 1998). In this system, proteins are targeted for degradation by covalent attachment with ubiquitin, a highly conserved small protein. The ubiquitin-protein conjugation requires the sequential actions of three enzymes (see Figure II). Initially, the C-terminal Gly residue of ubiquitin is activated in an ATP-dependent manner by a specific activating enzyme, E1. This step consists of an intermediate formation of ubiquitin adenylate, with the release of PPi, followed by the binding of ubiquitin to a Cys residue of E1 via a thiolester linkage, with the release of AMP. Activated ubiquitin is next transferred to an active site Cys residue of a ubiquitin-carrier protein, E2. In the third step, ubiquitin is catalyzed by a ubiquitin-protein ligase or E3 enzyme, then is linked to substrate proteins through an isopeptide bond between the C-terminal Gly and ε-amino group of the Lys in the substrates. Proteins conjugated with polyubiquitin chains are degraded by the 26S proteasome. Degradation by the ubiquitin-proteasome system regulates various cellular events such as the cell cycle, signal transudation, and maintaining the integrity of the proper folded state of

proteins.

Recently, several new ubiquitin-like modification systems have been discovered (Hochstrasser, 2000). These are utilized in the various kinds of reaction involving the ubiquitin-like proteins that modify substrates for different purposes than does ubiquitin itself. Such discoveries have suggested that these conjugation systems serve as regulatory mechanisms in a variety of cellular processes.

Lysosomal protein degradation

Majority of intercellular proteins was degraded in the lysosome. The lysosome is the major catabolic compartment in eukaryotic cells and contains a range of hydrolases capable of degrading most cellular constituents. The lysosome is the terminal destination for endocytic, autophagic and secretory materials targeted for destruction. Lysosomal degradation is critical to many physiological processes, including the turnover of normal cellular proteins, disposal of abnormal proteins, down regulation of surface receptors, release of endocytosed nutrients, inactivation of pathogenic organisms, antigen processing and so on. In yeast cells, there are a few large vacuoles, which are equivalent to lysosome in mammalian cells.

Three pathways have been described for delivering proteins to the lysosome for degradation: chaperone-mediated autophagy, microautophagy and macroautophagy. Chaperone-mediated autophagy is the process in which substrates to be degraded are translocated across the lysosome/vacuole membrane and delivered into the lumen of the lysosome/vacuole (Schworer *et al.*, 1981; Mortimore *et al.*, 1989; Dunn, 1994). In microautophagy, degradation substrates are engulfed by lysosome directly (Ahlberg and Glaumann, 1985; Mortimore *et al.*, 1988). Macroautophagy, by contrast, degradation substrates are sequestered into autophagosomes and delivered to lysosomes (Dice, 1990; Terlecky *et al.*, 1992; Cuervo and Dice, 1996). Among these processes, macroautophagy is well studied in both yeast and mammals because it is the major pathway to the lysosome/vacuole.

II. Autophagy

Autophagy in mammalian cells

In 1959, De Duve *et al*. discovered the lysosome and reported that cells can sequester and digest portion of their own cytoplasm in lysosome (De Duve, 1959). Following this discovery, many observations demonstrated that macroautophagy (referred to as autophagy simply hereafter) is responsible for this process (Ashford *et al*., 1962).

Autophagy is a membrane trafficking process that transports bulk cytoplasm and entire organelles to the lysosome for recycling (Figure I). The well-known triggers to induce autophagy are nutrient starvation (Mortimore and Poso, 1986) and hormones such as glucagon (Schworer CM. *et al*., 1979). This process involves the formation of a double-membrane structure, called autophagosome. At the first step, cytoplasmic components are enwrapped by a membrane sac called isolation membrane. Closure of the isolation membrane results in formation of autophagosome. Autophagosomes then fuse with endosomes, and eventually fuse with lysosomes. Lysosomal hydrolases degrade the cytoplasm-derived components of the autophagosome, together with its inner membrane.

Much of the knowledge of mammalian autophagy comes from morphological studies of liver cells or cultured cells by electron microscopy. The molecular basis of autophagy, however, has remained hidden for a long time, because mammalian lysosomes are too dynamic and complicated to analyze biochemically. The discovery of yeast autophagy proved to be a major turning point.

Discovery of Autophagy in yeast.

In 1992, Ohsumi and colleagues reported that the bulk protein degradation induced by starvation in the yeast *Saccharomyces cerevisiae* is mediated by autophagy, which is a similar process seen in mammalian cells (Takeshige *et al*., 1992). Autophagy in yeast is induced by nutrient limitation. Electron microscopic analysis found that autophagosomes bound by a double membrane appeared in the cytoplasm when yeast cells were starved (Baba *et al*., 1994). The autophagosome fused with the vacuolar membrane, allowing the release of its inner membrane into

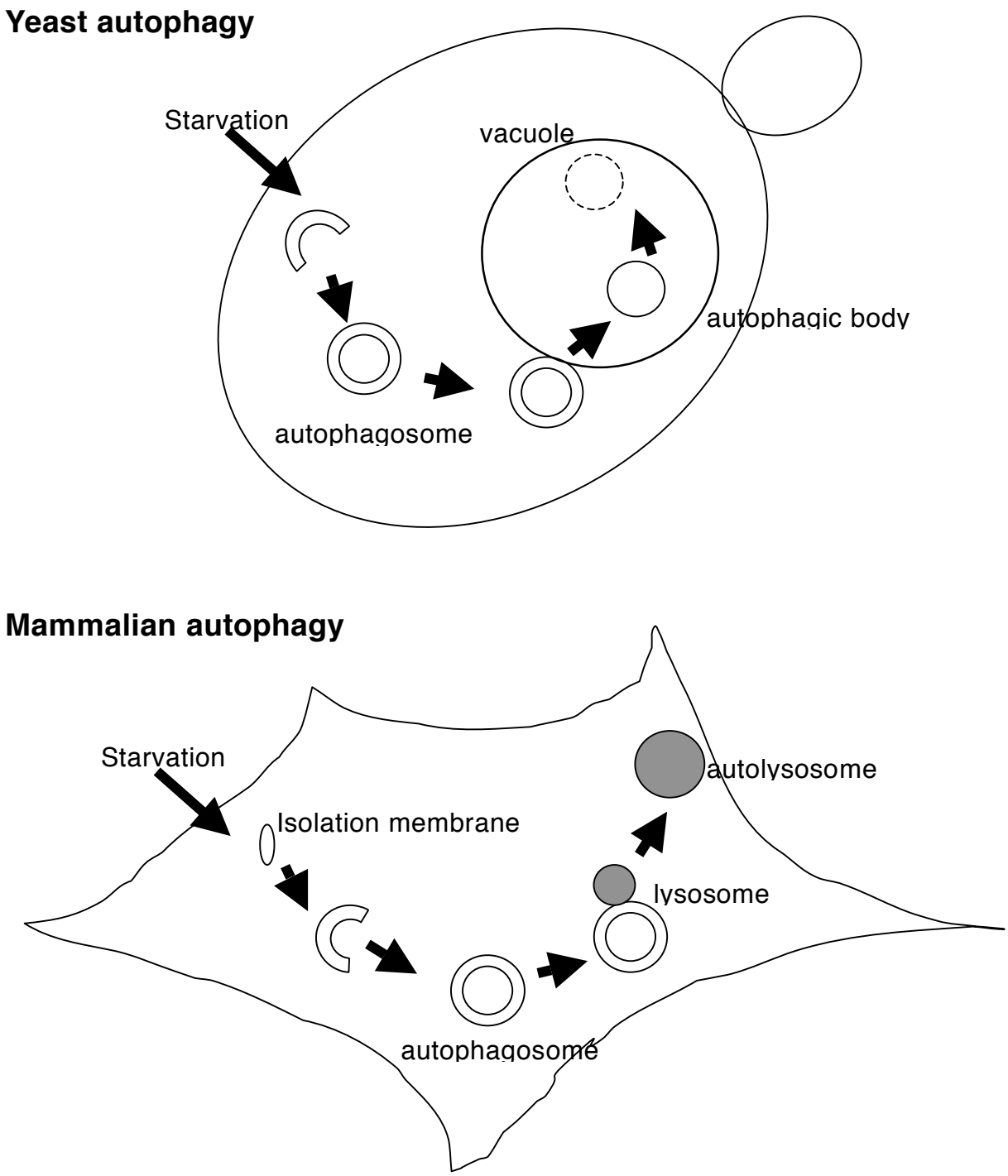

Figure I Membrane dynamics in autophagy

the vacuole lumen. The released materials are immediately degraded by vacuolar proteases. In mutants lacking vacuolar proteases, however, these released structures, named autophagic bodies, accumulate in the vacuole (Takeshige *et al.*, 1992). Electron microscopic analysis revealed that these autophagic bodies are mostly single-membrane structures containing a portion of cytoplasm (Baba *et al.*, 1995), indicating that starved yeast cells take up their own cytoplasm into vacuoles. The whole process in yeast is topologically the same as autophagy in mammals.

III.Molecular study on autophagy

Isolation of apg mutants

The discovery of autophagy in yeast introduced genetic approaches into this research field. Autophagy-defective mutants were obtained mainly by two-groups using different methods. Ohsumi and colleagues found that starved yeast cells accumulated autophagic bodies in the vacuole in the presence of PMSF, a serine protease inhibitor (Takeshige *et al.*, 1992). It was presumed that the inhibition of vacuolar proteolysis leads to an inability to break down vesicles that were derived form the autophagic transport. Therefore, in yeast, the process of autophagy can be monitored in real time by observing the accumulation of autophagic bodies in the vacuole by light microscopy. Using morphological screens for mutants unable to accumulate autophagic bodies during starvation, many *apg* mutants were obtained (Tsukada and Ohsumi, 1993). These mutants comprise 14 complementation groups. Electron microscopic analysis showed that the *apg* mutants do not accumulate autophagosomes in the cytoplasm, suggesting that all *apg* mutants have defects at or before formation of autophagosome.

The other genetic approach to identify autophagy mutants relied on the biochemical detection of the decrease of fatty acid synthase following starvation (Thumm *et al.*, 1994). This cytosolic enzyme is effectively degraded in the vacuole by autophagy. Mutants could not degrade the enzyme, resulting accumulation of fatty acid synthase. Utilizing this phenotype, *aut* mutants were isolated. The morphological and biochemical methods provided at least 16 genes (*APG* and *AUT* gene) involved in autophagy.

API transport to vacuole

An independent genetic screen in yeast led to the discovery of a genetic overlap between autophagy and the biosynthetic transport of a vacuolar hydrolase, aminopeptidase I (API) (Harding *et al.*, 1996; Scott *et al.*, 1996). API is known to be transported independently of the secretory pathway, by the cytoplasm-to-vacuole targeting (Cvt) pathway (Klionsky *et al.*, 1992). All *apg* mutants except one are shown to be defective in the Cvt pathway (Tsukada and Ohsumi, 1993), indicating that autophagy and the Cvt pathway share common molecular mechanisms.

Ubiquitin-like conjugation system

At the present, 15 *APG* genes were isolated in *Saccharomyces cerevisiae*. Recent studies on the Apg proteins have demonstrated that two-novel ubiquitin-like conjugation systems are essential for autophagy (Figure II). The first is the Apg12 conjugation system (Mizushima *et al.*, 1998a). Apg12 is a 186-amino acid protein without apparent homology to known proteins. Intriguingly, Apg12 is conjugated to another protein, Apg5. The mode of conjugation of Apg12 to Apg5 is quite similar to that of ubiquitin. The carboxy-terminal residue of Apg12 is glycine, which is activated by Apg7 in an ATP-dependent manner (Mizushima *et al.*, 1998a). Then, Apg12 forms a conjugate with Apg7 through a high-energy thioester bound (Tanida *et al.*, 1999; Kim *et al.*, 1999; Yuan *et al.*, 1999). Apg7 shows homology with E1 ubiquitin-activating enzyme within the region encompassing the putative ATP-binding site (GxGxxG) and the active site cystein (Mizushima *et al.*, 1998a). Most Apg7 exist as homo-dimer (Komatsu *et al.*, 2001). Apg12 is then transferred to Apg10 to form a thioester again (Shintani *et al.*, 1999). The function of Apg10 is likely equivalent to that of E2 ubiquitin-conjugation enzymes, although Apg10 has no homology to E2 enzymes. Finally, the carboxy-terminal glycine of Apg12 is covalently attached to lysine 149 of Apg5 via an isopeptide bond between the carboxyl group of the glycine residue and the □-amino group of the lysine residue (Mizushima *et al.*, 1998a). Formation of the Apg12-Apg5 conjugate is essential for proceeding of autophagy. This conjugation system is highly conserved in various eukaryotes (Mizushima *et al.*, 1998b).

The second is the Apg8 system (Figure II). Apg8 (also known as Aut7) is

Ubiquitin system

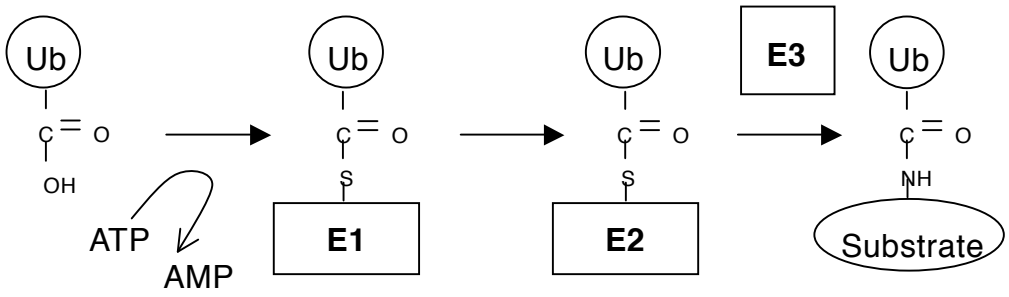

Apg12-Apg5 conjugation system

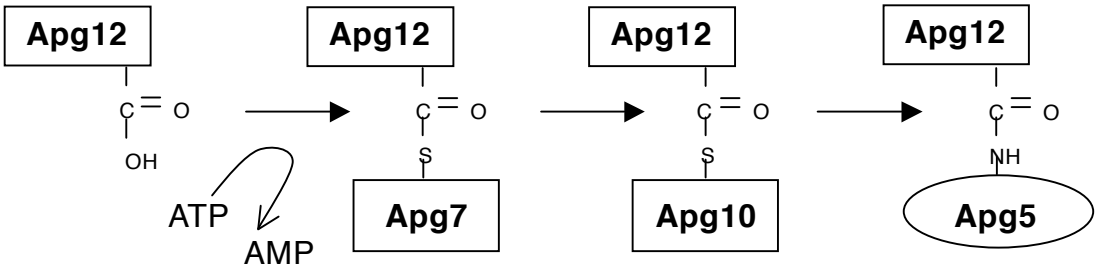

Apg8-PE conjugation system

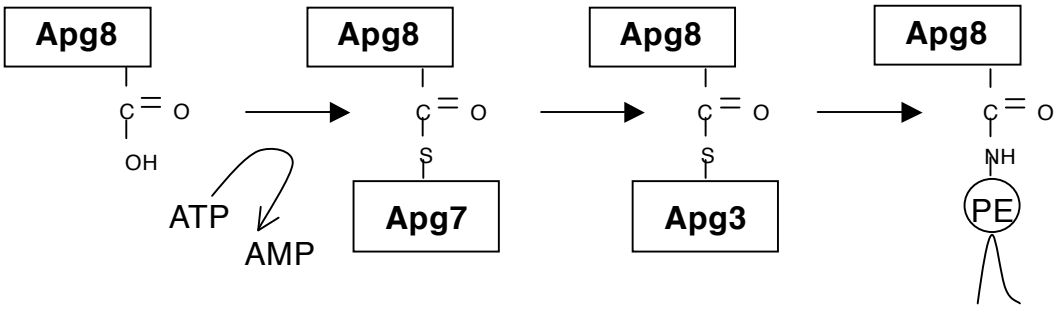

Figure II Ubiquitin-like conjugation systems

the first molecule found to localize to autophagosome (Kirisako *et al.*, 1999). The C-terminal arginine residue of Apg8 is cleaved off by Apg4/Aut2, a novel cystein protease (Kirisako *et al.*, 2000). The exposed glycine residue of Apg8 is conjugated to phosphatidylethanolamine (PE), which is catalyzed by Apg7 and Apg3/Aut1 (Ichimura *et al.*, 2000). Apg7 is shared with the Apg12 system whereas Apg3 is a specific conjugating enzyme for the Apg8 system. Subsequently, Apg8-PE is deconjugated again by Apg4. The cycle of conjugation and deconjugation is important for normal progression of autophagy (Kirisako *et al.*, 2000).

Recent studies suggest that these two ubiquitin-like systems function closely, probably have a direct linking. In the yeast cells defective in the Apg12 conjugation system, PE-conjugation of Apg8 is severely reduced (Suzuki *et al.*, 2001), and Apg12-Apg5 is immunoprecipitated with Apg8 (Kim *et al.*, 2002) (Dr. Suzuki, unpublished data).

Recently, it was demonstrated that both the Apg12 and Apg8 system are highly conserved in mammals (Mizushima *et al.*, 1998b). In mouse and human, there is only one orthologue for each component of the Apg12 system. While, at least three Apg8 homologues were identified in mammals: LC3 (Mann and Hammarback, 1994), GATE-16 (Sagiv *et al.*, 2000) and GABARAP (Wang *et al.*, 1999).

The role of Apg12-Apg5 conjugate in autophagosome formation.

The significance of the Apg12-Apg5 conjugate has been shown in several experiments in both yeast and mammalian cells. Studies using yeast cells deficient in *APG5* or temperature sensitive mutant showed that Apg5 is directly required for autophagosome formation (George *et al.*, 2000). Morphological observation demonstrated that most yeast Apg5 exists diffusely in the cytoplasm, and a small portion localizes to the pre-autophagosomal structure (PAS) (Suzuki *et al.*, 2001). In yeast, autophagosomes seem to be generated from PAS, a structure near the vacuole, to which multiple Apg proteins, Apg1, Apg2, Apg8, Apg9, the Apg12-Apg5 conjugate, Apg14 and Apg16 are targeted (Kim *et al.*, 2002; Suzuki *et al.*, 2001) (Figure III).

Similarly, in mouse embryonic stem (ES) cells, the Apg12-Apg5 conjugate

is targeted from the cytoplasm to the isolation membrane during autophagosome formation (Figure III). It was observed that Apg12-Apg5 conjugate initially associates with a small crescent-shaped vesicle evenly. As the membrane elongates, Apg12-Apg5 associates with the outer side of the membrane asymmetrically. Finally, Apg12-Apg5 dissociates from the membrane upon completion of autophagosome formation. It is not known whether the autophagosome precursor is equivalent to PAS seen in yeast cells. LC3, a homologue of yeast Apg8, was shown to localize on autophagosome membrane. LC3 remains on autophagosome even after Apg12-Apg5 conjugate dissociates, so that it is used as a autophagosome maker. It has not confirmed whether GATE-16 and GABARAP, the other homologues of Apg8, localized in autophagosome yet.

Analysis using the mouse Apg5^{K130R} mutant protein, which is unconjugated with Apg12, demonstrated that Apg12-Apg5 is required for elongation of the isolation membrane to form a complete spherical autophagosome (Mizushima *et al.*, 2001). The Apg12-Apg5 conjugate is also required for association of LC3 with pre-autophagosome membranes also in mammalian cells (Mizushima *et al.*, 2001). These results suggest that the Apg12-Apg5 conjugate plays an essential role in isolation membrane development together with Apg8/LC3, but the exact molecular role of the Apg12-Apg5 conjugate has not been elucidated yet.

Yeast Apg16, an interacting protein with the Apg12-Apg5 conjugate.

Yeast Apg16 is the only molecule thus far identified to interact with the Apg12-Apg5 conjugate. It was originally obtained by a two-hybrid screen using Apg12 as bait and was found to interact with the Apg12-Apg5 conjugate. Following experiments showed that Apg16 interacts directly with Apg5 but not with Apg12. Apg16 is a 150-amino acid protein (17 kDa) that contains a carboxyl-terminal coiled-coil motif (residues 58-123) and associates with Apg5 at its amino-terminal region (see Fig.11).

In *apg16* deletion mutant, autophagosomes were not formed, even though the Apg12-Apg5 conjugate was normally formed (Mizushima *et al.*, 1999). Targeting of the Apg12-Apg5 conjugate to PAS is dependent on Apg16 (Suzuki *et al.*, 2001; Kim *et al.*, 2002). These data suggest that Apg16 is essential for the

function of Apg12-Apg5 conjugate. Previous study demonstrated that Apg16 forms an oligomer through the coiled-coil region and cross-links Apg12-Apg5 conjugates (Mizushima *et al*., 1999).

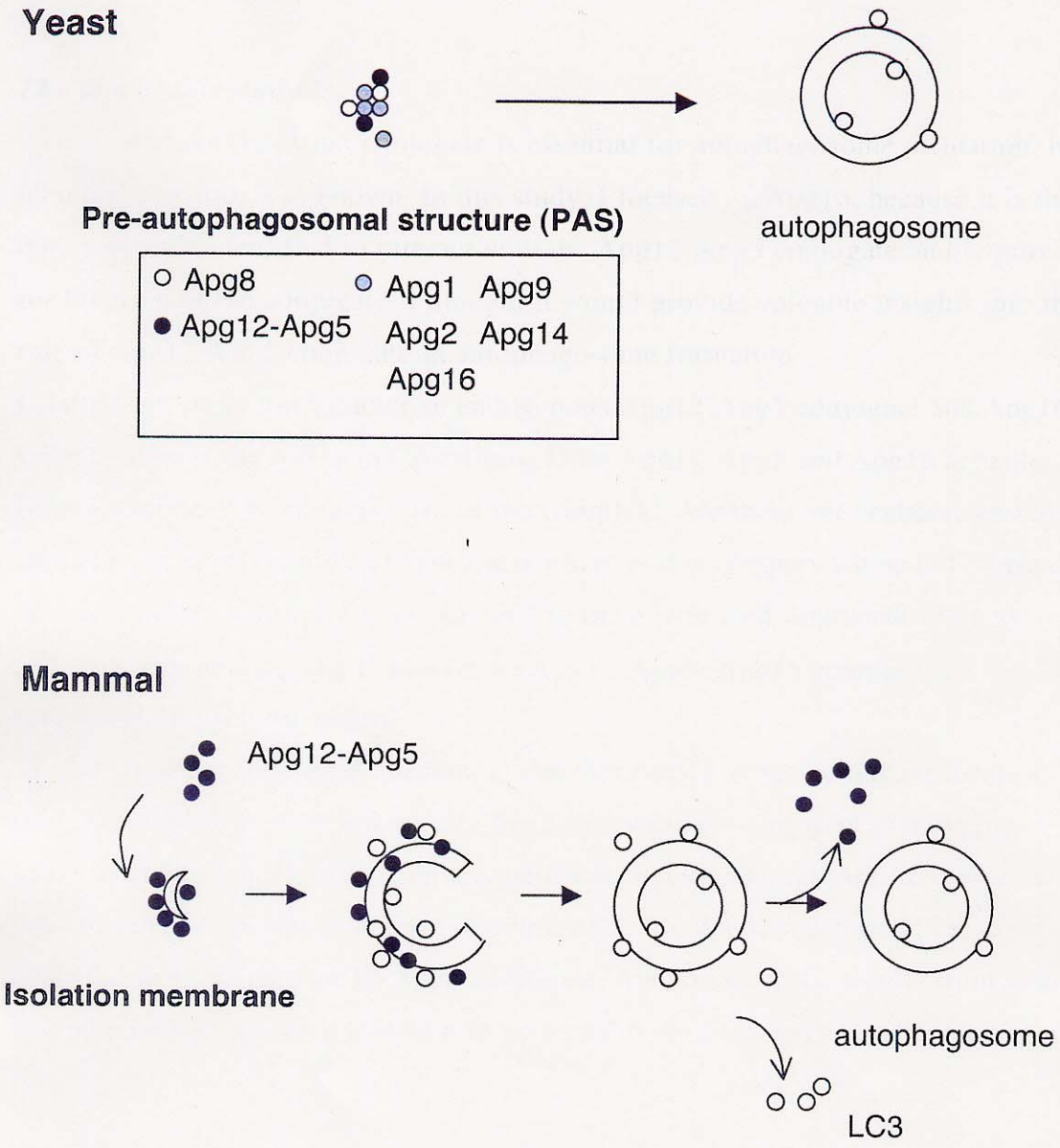

Figure III Scheme of the autophagosome formation in yeast and mammalian cells.

It suggests that Apg12-Apg5 conjugate and Apg16 form a large protein complex through Apg16-oligomer, although it has not been determined.

The aim of this study.

The Apg12-Apg5 conjugate is essential for autophagosome formation, but its molecular role is unknown. In this study, I focused on Apg16, because it is the only molecule identified to interact with the Apg12-Apg5 conjugate and required for function of the conjugate. I thought it would provide valuable insights into the role of Apg12-Apg5 conjugate in autophagosome formation.

I started my study to characterize endogenous Apg12-Apg5 conjugate and Apg16 in yeast to answer the following questions. Dose Apg12-Apg5 and Apg16 actually form a complex? What is the size of the complex? Are there yet uncharacterized components in this complex? When and where is this complex formed? Is formation of this complex required for autophagy? Using a regulated oligomerization system and a gel filtrate analysis, I showed the Apg12-Apg5･Apg16 complex is a functional unit for autophagy.

Another important question is whether Apg12-Apg5 conjugate forms a protein complex in other eukaryotes, because there is no apparent homologue of yeast Apg16 in other spices from database search, even though Apg12 system is well conserved. To obtain a general solution of autophagic machinery, I also analyzed mammalian Apg12-Apg5 conjugate. A merging of the results from yeast and mammalian analyses will help to understand the autophagy machinery.

Material and Method

Yeast strains and media

The yeast strains used in this study were SEY6210 (*MATa his3-Δ200 leu2-3, 112 lys2-801 trp1-Δ901 ura3-52 suc2-Δ9 GAL*) (Dawson *et al*., 1975), KVY115 (*MATa his3-Δ200 leu2-3, 112 lys2-801 trp-Δ901 ura3-52 suc2-Δ9 GAL Δapg12::HIS*), KVY117 (*MATa his-Δ200 leu2-3, 112 lys2-801 trp1-Δ901 ura3-52 suc-Δ9 GAL Δapg16::LEU2*), and KVY142 (*MATa his-Δ200 leu2-3, 112 lys2-801 trp1-Δ901 ura3-52 suc-Δ9 GAL Δapg5::LEU2*)(Suzuki *et al*., 2001). The other apg disruptants used in Fig. 1 were also created with SEY6210 (Suzuki *et al*., 2001). Cells were grown in either in YPD (1% yeast extract, 2% peptone, 2% glucose) medium or in SD medium containing nutritional supplements. For nitrogen starvation, SD (-N) medium (0.17% yeast nitrogen base without amino acids and ammonium sulfate, 2% glucose) was used.

Cell culture and transfections

R1 ES cells (a generous gift from Dr. Andras Nagy, Samuel Lunenfeld Research Institute, Toronto, Canada) were cultured on mytomycin C-treated embryonic fibroblasts or gelatinized dish in a complete ES medium: high glucose Dulbecco's modified Eagle's medium supplemented with 20% f*et al* bovine serum (SIGMA), 2mM L-glutamine, non-essential amino acids (GIBCO BRL), 1μM 2-mercaptoethanol, antibiotics and 1,000 U/ml leukemia inhibitory factor (Life technologies, INC.). The generation of Apg5-/- ES cells and various stable transformants have been described (Mizushima *et al*., 2001). HeLa cells were cultured in Dulbecco's modified medium (SIGMA) supplemented with 10% FCS. To starve cells of amino acid, cells were cultured in Hank's solution containing 10 mM Hepes, pH 7.5 (without amino acid and FCS). Transient transfections were performed using LipofectAMINE 2000 reagent (Life Technologies). Transfected cells were processed for immunobloting or immunoprecipitaion 18 hr after transfection. To obtain stable transformants, 8 x 10^6 ES cells were electroporated with 20 μg of linearized plasmid. Cells were selected in the presence of 1 mg/ml G418.

Plasmid construction

To create the glutathione S transferase (GST)-Apg12, GST-Apg16 and GST-Apg5 fusion constructs, the open reading frames (ORFs) of Apg12 and Apg16 were cloned into the blunted EcoRI and SmaI sites of pGEX-3X (Amersham Pharmacia Biotech) to yield pGEX-3X-Apg12 and pGEX-3X-Apg16, respectively. The Apg5 ORF was cloned into the BamHI site of pGEX-2T to generate pGEX-2T-Apg5. For expression of 6xHis-tagged Apg16, the Apg16 ORF was first cloned into the EcoRI site of pENT3C from the GATEWAY cloning system (Invitrogen). A 6xHis-Apg16-expression plasmid (pDEST17-Apg16) was then generated according to the manufacturer's instructions. To make the Apg16-2FKBP^{F36V} fusion constructs, we first created BamHI sites within the C-terminal coiled-coil region of Apg16 (after the amino acid residue 65 and/or 118), by mutagenizing pApg16, a pRS314 vector containing the APG16 gene (Mizushima *et al*., 1999), using the QuikChange^{TM} Site-directed Mutagenesis Kit (Stratagene). The fragment containing two tandem copies of FKBP^{F36V} was PCR-amplified from the plasmid pC4-Fv2E (provided by ARIAD Pharmaceuticals Inc.) with primers that were designed to have in-frame BamHI sites in their 5' ends: Fv2E5N 5'-ATCGGGATCCAGGCGTCCAAGTCGAAACCA-3' and FKBP 5'-GCATGGATCCGCGTAGTCTGGTACGTCGTACGG-3'. The resulting 2FKBP^{F36V} fragment was digested with BamHI and inserted into the mutated pApg16 plasmids, either into one of the two BamHI sites or between them, to generate pApg16^{65}-2FKBP^{F36V}, pApg16^{118}-2FKBP^{F36V} and pApg16$^{\Delta 65-118}$-2FKBP^{F36V}.

cDNA corresponding to the ORF of mouse Apg16L, was obtained by PCR of IMAGE consortium clone 1480862 (GenBank accession number AI037166). This fragment was then cloned into the SalI site of pCI-neo (Promega), the XbaI site of p3xFLAG-CMV-10 (SIGMA), the Sal sites of pEGFP-C1, pECFP-C1 and pEYFP-C1, to generate pCI-Apg16L, pFLAG-Apg16L, pEGFP-Apg16L, pECFP-Apg16L and pEYFP-Apg16L, respectively. The mouse Apg5 and rat LC3 cDNAs were also subcloned into pECFP-C1 (pECFP-Apg5) and pEYFP-C1 (pEYFP-LC3). To attain better expression in ES cells, the Apg16L, FLAG-Apg16L, EGFP-Apg16L, ECFP-Apg16L and EYFP-Apg16L fragments were also subcloned into pCE-FL (a

generous gift from Dr. S. Sugano), a vector containing a CMV enhancer and elongation factor promotor. pApg5-HA and pEGFP-Apg5. For yeast two-hybrid analysis, various regions of Apg16La cDNA corresponding to amino acid 1-588 (full length), 1-276, 1-79, 72-276 and 219-588 were cloned into the SalI site of pGBD-C1 and pGAD-C1. The mouse Apg5 cDNA was also cloned into the SmaI sites of pGBD-C1 and pGAD-C1. For screening, full length of Apg16L cDNA was cloned into the SalI site of pLexA-ADE2.

Antibodies

Antibodies against yeast Apg12, Apg16, Apg5 and mouse Apg16L were prepared as follows. The pGEX-3X-Apg12, pGEX-3X-Apg16 and pGEX-2T-Apg5 plasmids were transformed into *E.coli* XL1 Blue MRF', and transformants were grown in LB medium containing 50 □g/ml ampicillin to 0.5 OD_{600} pDEST15-Apg16CL was transfected into BL21-SI competent cells. Recombinant protein expression was induced with 1 mM isopropyl-□-D-thiogalactopyranoside or 0.3M NaCl during additional 3 hr-culture at 37 ˚C. The recombinant proteins in the inclusion bodies were separated by SDS-PAGE and simultaneously stained with Coomassie Brilliant Blue G250. The protein bands were cut off and eluted with elution buffer (100 mM Tris, pH 6.8, 0.05% SDS). The eluted proteins were used to immunize rabbits. Antiserum against Apg16 was subsequently affinity purified by passing serum over a column of 6xHis-tagged Apg16 recombinant protein coupled to CNBr-activated Sepharose 4B (Amersham Pharmacia Biotech). For expression of 6xHis-tagged Apg16, the pDEST17-Apg16 plasmid was transformed into BL21-SI competent cells, and transformants were grown up to 0.5 OD_{600} at 30 ˚C in LB without NaCl medium (1% bactotryptone, 0.5% yeast extract) containing 50 □g/ml ampicillin, and expression of 6xHis-Apg16 protein was induced for 2 hr with 0.3 M NaCl. 6xHis-tagged Apg16 was purified from inclusion bodies as described above. The purified His-Apg16 protein was covalently coupled to CNBr-activated sepharose, and incubated with antiserum overnight at 4 ˚C. After washing unbound antisera extensively, and bound antibodies were eluted with 0.1 M glycine, pH 2.8. Eluates containing the affinity-purified antibodies were neutralized and stored at -80 ˚C. Anti-Apg5 antibody was purified likewise using GST-Apg5-conjugated formyl-

cellulofine. Antiserum to AP was provided by Dr. Daniel J. Klionsky (University of Michigan).

Western blotting of total cell lysates

Yeast cell lysates were prepared as follows. Cells were grown to 1 OD_{600} unit/ml and, if necessary, starved for 3 hr in SD (-N) medium. Ten OD_{600} units of cells were harvested by centrifugation and directly resuspended in 100 l of a solution containing 0.2 M NaOH and 0.5% 2-mercaptoethanol. Cells were incubated for 15 min on ice, after which 1 ml of cold acetone was added, and the cells were incubated further for 30 min at -20 ˚C. After centrifugation at 15,000 x *g* for 5 min, pellets were resuspended in 200 l SDS-sample buffer and boiled for 5 min. Lysates were subjected to SDS-PAGE and immunoblotting.

Lysates from HeLa and ES cells were prepared as follows. Cells grown on 35 mm dishes were washed with PBS and lysed in lysis buffer (2% NP-40 in PBS supplemented with protease inhibitor) for 20 min on ice. The cellular debris was cleared by centrifugation, and the supernatants were subjected to western blotting.

Differential centrifugation

Yeast cells were grown to 1 OD_{600} unit/ml, and 50 OD_{600} units of cells were collected by centrifugation. Spheroplasts were generated and lysed by Dounce homogenization in lysis buffer (20 mM PIPES, pH 6.8, 5 mM $MgCl_2$, 100 mM sorbitol and protease inhibitors) with or without 150 mM NaCl. After a preclearing step at 100 x *g* for 5 min, the lysates were subjected to low-speed centrifugation at 13,000 x *g* for 20 min to generate a pellet (P13) fraction. The resulting supernatant was further centrifuged at 100,000 x *g* for 1 hr to generate pellet (P100) and supernatant (S100) fractions.

ES cells were lysed in lysis buffer (50 mM Tris-HCl, pH7.5, 150 mM NaCl and protease inhibitors) by passing the solution through a polycarbonate filter with 5- m pore (Whatman). The following steps were the same as above.

Gel filtration

S100 fractions prepared form yeast cells, ES cells and mouse tissue homogenates

were separated by size exclusion chromatography on a Superdex 200 column or a Superose 6 column (Amersham Pharmacia Biotech). The liver and brain of a C57BL/6N Crj mouse were homogenized in nine volumes of ice-cold PBS supplemented with protease inhibitor and centrifuged at 100,000 x g for 1h. The resulting supernatants (0.3~ 0.4 mg protein in 200 μl) were applied to and eluted from the columns at a flow rate of 0.5 ml/min with 50 mM Tris, pH 6.8, 150 mM NaCl, 1 mM DTT. Fractions were collected and then examined by immunoblotting. The column was calibrated with both HMW and LMW gel filtration protein standards (Amersham Pharmacia Biotech) containing thyroglobulin (*M*r =669 kDa), ferritin (*M*r=440 kDa), catalase (*M*r=232 kDa), aldolase (*M*r=158 kDa), albumin (*M*r=67 kDa), ovalbumin (*M*r=43 kDa) and chymotrypsinogen A (*M*r=25 kDa).

In vivo labeling and immunoprecipitation

Yeast cells were incubated in SD medium without methionine overnight, and then labeled with 0.5 mCi of [^{35}S] methionine/ cysteine (NEN Life Scienece Products) for one hour. Cells were collected by centrifugation and converted to spheroplasts. Sheroplasts were lysed in IP-lysis buffer (50 mM Tris-HCl, pH 7.5, 150 mMNaCl, 5 mM EDTA, 5 mM EGTA, 1mM PMSF and 1 x protease inhibitor mixture (CompleteTM; Boehringer Mannheim)) by passing the solution through a polycarbonate filter with 5-μm pore (Whatman). After removal of cell debris by brief centrifugation, the lysates were solubilized with 0.1 volume of 10% Nonidet P-40. The lysates were incubated with anti-Apg12 antibody at 4˚C for 2 hr, and then Protein A Sepharose were added and incubated additional 2 hr. Immunoprecipitates were washed 6 times in IP-lysis buffer containing 1% NP-40 and eluted in SDS sample buffer. Proteins were separated by SDS-PAGE and analysed by either a bioimage analyser BAS2000 (Fuji Film).

ES cells grown on 35 mm dishes were labeled with 0.4 mCi of [^{35}S] methionine/cysteine for two hours when indicated. After cells were lysed in lysis buffer (2% NP-40 in PBS supplemented with protease inhibitor) for 20 min, the nuclear and cellular debris was cleared by centrifugation. Immunoprecipitation was performed using rabbit polyclonal anti-GFP (MBL), mouse monoclonal anti-FLAG (M2)(SIGMA) or anti-HA antibody (16B12)(BabCO) and protein A- or Protein G-

sepharose (Amersham Bioscience). The following steps were the same as above.

Regulated oligomerization analysis

The pC4-Fv2E plasmid that contains two tandem copies of $FKBP^{F36V}$ and the bivalent ligand AP20187 were kindly provided by ARIAD Pharmaceuticals Inc. (http://www.ariad.com/regulationkits). For induction of oligomerization, Δ*apg16* cells expressing Apg16-$2FKBP^{F36V}$ were cultured overnight in appropriate medium containing 0.1 μM AP20187.

Protein purification and mass spectrometry

Total cell lysates were prepared from ten to twenty 15 cm dishes of ES cells. The protein complex containing GFP5-Apg5 was purified by passing the lysates over an anti-GFP antibody-coupled protein A-Sepharose beads column. After extensive washing, bound proteins were eluted in 0.1 M glycine-HCl (pH 2.5), separated by SDS-PAGE and visualized with Coomassie Brilliant Blue or silver staining. Following excision from the gels, proteins of 63 kDa and 71 kDa were digested in situ with lysyl-endpeptidase or trypsin. The resultant peptides were subjected to matrix-assisted laser desorption ionization (MALDI)-mass spectrometry. Proteins were identified by database searching based on their peptide masses. For further unambiguous protein identification, the same bands were digested with lysyl-endopeptidase and then analysed by the direct nano LC-MS/MS system (Natsume *et al.*, 2002) in conjunction with searches of the NCBI nr database using Mascot software.

RT-PCR

Total RNA, isolated from mouse liver, brain, kidney, ES cells and HeLa cells, was subjected to reverse-transcription using a ProSTARTM First-strand RT-PCR kit (Stratagene). A part of the Apg16L cDNA corresponding to exon 6-10 was amplified with primer p63-4Bam (5'- ACGTGGATCCAGGAGGCGTCAAGCACGGCTG-3') and p63-22Sal (5'- GAACGTGTCGACCTGGGGGACTGGGATGGAAGAGAC-3').

Yeast two-hybrid assay

The two-hybrid analysis was performed as described (James *et al.*, 1996). The strains PJ69-4A or L40 were co-transformed with one of each of the pGBD, pGAD and pLexA-ADE2 plasmids. Transformants were selected on Trp^- Leu^- plates and tested for growth on His^- Trp^- Leu^- plates containing 3 mM 3-amino-triazole.

Fluorescence microscopy

ES cells expressing GFP-, YFP-, CFP-fused protein were directly observed with a DeltaVision microscope system (Applied Precision Incorporation). For examination by immunofluoresence microscopy, ES cells grown on gelatinized coverslips were fixed and stained with an anti-mouse Apg16L antibody (200 x dilution) and a Cy5-conjugated goat anti-rabbit IgG antibody (Amersham Bioscieneces). Samples were examined under a fluorescence lase scanning confocal microscope, LSM510 (Carl Zeiss) as previously described (Yoshimori *et al.*, 2000)

Results

I. Analysis of yeast autophagy

Characterization of endogenous Apg12-Apg5 conjugate and Apg16.

Using the yeast *Saccharomyces cerevisiae*, I first examined the state of the Apg12-Apg5 conjugate by immunoblot analysis using anti-Apg12 antibody. Most endogenous Apg12 exist in the form of conjugate with Apg5 in wild-type cells (Fig. 1). This is true in *apg* mutants except for Δ*apg5*, Δ*apg7* and Δ*apg10*. In these three *apg* mutants, which are defective in Apg12 conjugation (Mizushima *et al.*, 1998a), Apg12 was present exclusively in the unconjugated form. The amounts of Agp12-Apg5 conjugates and unconjugated Apg12 did not change during nitrogen starvation (data not shown). I next examined the subcellular distribution of the endogenous Apg12-Apg5 conjugate by differential centrifugation (Fig. 2). Previous studies demonstrated that distribution of the hemagglutinin (HA) epitope-tagged Apg12-Apg5 conjugate depends on lysis buffer conditions (Mizushima *et al.*, 1999; George *et al.*, 2000). Thus, I tested four different buffer conditions. The constitution of buffers is described in Fig. 2. Yeast spheroplasts were homogenised with each lysis buffer. After removal of cell debris, the lysates were centrifuged at 13 k x *g* for 20 min to generate a pellet (P13) fraction. The resulting supernatant was centrifuged again at 100 k x *g* for 1 hr to further separate it into pellet (P100) and supernatant (S100) fractions. Each fraction was subjected to immunoblotting with anti-Apg12 antibody. The distribution of the endogenous Apg12-Apg5 conjugate was considerably affected by the salt concentration of the lysis buffer. In buffer containing 150 mM NaCl, the Apg12-Apg5 conjugate was found primarily in the S100 fraction, whereas in the absence of salt it was mainly found in the P100 fraction (Fig. 2). Since the distribution when salt-containing buffer was used is more consistent with the morphological observations that most Apg5 is distributed throughout the cytoplasm in both yeast and mammalian cells (Suzuki *et al.*, 2001; Mizushima *et al.*, 2001), buffer containing physiological salt concentrations was used in the following experiments. The distribution of Apg12-Apg5 conjugate was not changed during nitrogen starvation (Fig. 3)

I performed the same experiment for Apg16 because it was known to interact

with Apg12-Apg5 conjugate. First, I purified anti-Apg16 antibody, which were prepared by Dr. Ishihara, using recombinant Apg16-conjugated column to analyze endogenous Apg16. With this affinity-purified antibody, Apg16 was detected at the expected molecular size (Fig. 4). When Apg16 was overexpressed, an additional band (* in Fig. 4) was observed as previously reported (Mizushima *et al.*, 1999), although it has not yet been characterized. Apg16 displayed a distribution pattern similar to that of Apg12-Apg5 (Fig. 5).

Cytosolic Apg12-Apg5 conjugate and Apg16 form a ~350-kDa complex.

A previous study suggested that Apg16 forms an oligomer and cross-links the Apg12-Apg5 conjugates (Mizushima *et al.*, 1999), although it has not been determined. To characterize the Apg12-Apg5·Apg16 complex, I performed gel filtration analysis. The S100 fraction was subjected to gel filtration analysis using a Superdex 200 column and subsequently immunoblotted with anti-Apg12 and anti-Apg16 antibodies. The Apg12-Apg5 conjugate mainly eluted in a single peak in fractions corresponding to ~ 350 kDa (Fig. 6). Most Apg16 was also recovered in these fractions. Co-elution of Apg12-Apg5 and Apg16 indicates that most of the Apg12-Apg5 conjugate and Apg16 form a ~350-kDa protein complex. Monomeric Apg12-Apg5 conjugate and Apg16 were scarcely detected. The ~350-kDa complex was already formed under nutrient conditions and the elution profile was not affected by nitrogen starvation (Fig. 6). In contrast, in Δ*apg16* cells, the ~350-kDa complex was not observed and the Apg12-Apg5 conjugate was found in ~60-kDa fractions which corresponds to the sum of the molecular weights of Apg12 (21 kDa) and Apg5 (33 kDa) (Fig. 7a). Although Apg16 was expected to cross-link two Apg12-Apg5 conjugates (Mizushima *et al.*, 1999), the size of the resulting complex was significantly larger than what would be expected from two sets of Apg12-Apg5·Apg16. One possible explanation is that there may be additional components. However, as far as I examined by immunoprecipitation analysis using anti-Apg12 antibody, I could not detect any protein other than Apg12, Apg5 and Apg16 (Fig. 8). I further examined whether Apg8 and Apg3 were contained in the ~350-kDa complex by gel filtrate analysis, because both were suggested to be co-precipitated with Apg12-Apg5 conjugate (Kim *et al.*, 2002)(Dr. Suzuki, unpublished data) and

functional relationship between the Apg8 and Apg12 systems were observed (Suzuki *et al.*, 2001; Mizushima *et al.*, 2001). As a result, Apg8 mainly eluted in single peak in fractions corresponding to less than 20-kDa, which would represent monomeric Apg8 (MW=14 kDa). Apg3 eluted primarily in fractions corresponding to ~60 kDa, with a minor peak in ~250 kDa fraction. Although the elution peak position of Apg3 was larger than molecular size of Apg3 (MW=36 kDa), it was not characterized in this study. Thus, I concluded that neither Apg8 nor Apg3 are included in the ~350-kDa complex. Furthermore, my observation that the main Apg12-Apg5 conjugate peak was shifted to fractions much smaller than half of 350 kDa in Δ*apg16* cells (Fig. 7a) suggests that the ~350-kDa complex is not dimeric. Therefore, I believe the ~350-kDa complex represents an Apg12-Apg5·Apg16 multimeric complex, most probably tetrameric, the formation of which is mediated by Apg16 oligomerization.

I also performed gel filtration analysis on Δ*apg5* and Δ*apg12* cells. In Δ*apg5* cells, the ~350-kDa complex was not present, and the Apg12 and Apg16 peaks were detected in fractions of low molecular size (Fig. 7b). The eluting peak position of Apg16 (fractions 11 and 12) was larger than the expected molecular size of Apg16 monomer. When I performed gel filtration analysis using Δ*apg5*Δ*apg16* cells expressing both ^{Myc}Apg16 and ^{HA}Apg16, the tagged Apg16 was recovered in the same fractions (data not shown). Co-immunoprecipitation analysis revealed that the amount of ^{Myc}Apg16-^{HA}Apg16 dimer was very little and most Apg16 existed as a monomer in the absence of Apg5 (data not shown), suggesting that Apg16 in fractions 11 and 12 represents monomeric form. Apg16 might not be a globular protein and behave aberrantly in size exclusion chromatography. Taken together, these results suggest that the Apg5-Apg16 interaction would be important for Apg16 to form an oligomer. In contrast, in Δ*apg12* cells, Apg5 and Apg16 were mainly co-eluted in ~250-kDa fractions, which would represent the complex made up of four sets of Apg5 and Apg16 (Fig. 7c). Therefore, even in the absence of Apg12, Apg5 and Apg16 could form the tetrameric complex.

To confirm that formation of the ~350-kDa complex is mediated by Apg16, I reconstituted the complex formation using two different cell lysates: one was prepared from Δ*apg16* cells, in which the Apg12-Apg5 conjugate existed as a

monomeric form (Fig. 10a), and the other was from Δ*apg5*Δ*apg12* cells overexpressing Apg16, in which most Apg16 was monomeric (Fig. 10b). These two cell lysates were mixed, incubated at 4°C overnight and subjected to gel filtration analysis. In contrast to the pre-mixed sample (Fig. 10a), the ~350-kDa complex was clearly detected in the incubated mixture (Fig. 10c). I also observed a small but significant shift of the Apg12-Apg5 fractions after 1 hr-incubation of the lysates (data not shown).

Apg16-oligomerization is required for the ~350-kDa Apg12-Apg5·Apg16 complex formation.

Because the above experiments suggested that formation of the ~350-kDa complex is mediated by Apg16 homo-oligomer (Fig. 11), I next attempted to control the oligomerization state of Apg16 in order to determine whether the formation of this complex is required for Apg16-oligomerization. I employed a regulated oligomerization system, which allows drug-induced multimerization of proteins of interest (Amara *et al.*, 1997; Clackson *et al.*, 1998) (Fig.12). This system is based on FK506 binding protein (FKBP) and its small ligand FK506. A bivalent drug AP20187, which is created by chemically linking two FK506 derivatives, is able to cross-link fusion proteins containing the $FKBP^{F36V}$ domain, in which Phe36 of wild-type FKBP is replaced with valine. AP20187 has 1000-fold higher affinity for $FKBP^{F36V}$ than for wild-type FKBP. Thus, a fusion protein containing two copies of $FKBP^{F36V}$ is capable of forming oligomers in the presence of AP20187. Since Apg16 is suggested to form an oligomer through its C-terminal coiled-coil region (Fig. 11) (Mizushima *et al.*, 1999), I modified Apg16 by inserting two tandem copies of $FKBP^{F36V}$ after amino acid 65 or 118 (described as $Apg16^{65}$-2$FKBPF^{36V}$ and $Apg16^{118}$ -2$FKBP^{F36V}$, respectively), or by using it to replace nearly the entire the coiled-coil region ($Apg16^{\Delta 65\text{-}118}-2FKBP^{F36V}$), where they would disrupt the coiled-coil region and thereby inhibit natural Apg16 oligomerization (Fig.13). I then tested whether each Apg16-2$FKBP^{F36V}$ fusion protein oligomerized in an AP20187-dependent manner. Δ*apg16* cells expressing each Apg16-2$FKBP^{F36V}$ fusion protein were treated with or without 0.1 μM of AP20187 and cell lysates were separated on a Superdex 200 column as described above. Among these constructs, only the

Apg16^{65}-2FKBP^{F36V} fusion protein, which was inserted with 2FKBP^{F36V} immediately after the beginning of the coiled-coil region allowed for ligand dependent oligomerization. The Apg16^{118} -2FKBP^{F36V} fusion protein formed oligomer irrespective of the AP20187 treatment and the Apg16$^{\Delta 65\text{-}118}$-2FKBP^{F36V} was not evaluated because of its low expression. Without AP20187, the Apg16^{65}-2FKBP^{F36V} was detected in fractions corresponding to ~200 kDa (Fig. 14a). In this peak, Apg16^{65}-2FKBP^{F36V} associated with Apg12-Apg5 conjugate, because Apg16^{65}-2FKBP^{F36V} was detected at ~55 kDa in Δ*apg5* cells, which was probably monomeric Apg16^{65}-2FKBP^{F36V} (Fig. 14b). Since the sum of the molecular weights of Apg12, Apg5 and Apg16^{65}-2FKBP^{F36V} is about 100 kDa, my data suggest that dimeric Apg12-Apg5·Apg16^{65}-2FKBP^{F36V} could be formed even in the absence of AP20187. The remaining coiled-coil region of Apg16^{65}-2FKBP^{F36V} might function partially (see discussion). After AP20187-treatment, the peak of Apg16^{65}-2FKBP^{F36V} was clearly shifted to fractions corresponding to ~400 kDa (Fig. 14c). This change of peak indicates that Apg16 oligomerizes upon AP20187 treatment.

Using this controlled Apg16 oligomerization system with the Apg16^{65}-2FKBP^{F36V} construct, I examined the complex state of the Apg12-Apg5 conjugate. In the absence of AP20187, the Apg12- Apg5 conjugate was mainly eluted at ~60 kDa, equivalent to the molecular mass of the conjugate (Fig. 14b). After treatment with AP20187, Apg12-Apg5 conjugate was found to elute in ~400-kDa fractions (Fig. 14d), together with oligomerized Apg16^{65}-2FKBP^{F36V}. This peak corresponds to the wild-type ~350-kDa Apg12-Apg5·Apg16 complex; insertion of 2FKBP^{F36V} (about 24 kDa) into Apg16 accounts for the difference. These results suggest that formation of the ~350-kDa Apg12-Apg5·Apg16 complex requires Apg16 oligomerization, and that I was effectively able to regulate the formation of the complex with this AP20187-dependent oligomerization system.

The ~350-kDa complex is required for autophagy.

Next, I determined whether the formation of the ~350-kDa complex is necessary for autophagy using the oligomerization system. Δ*apg16* cells expressing Apg16^{65}-2FKBP^{F36V} were incubated with AP20187 overnight and then starved with nitrogen-free medium containing 1 mM PMSF and 0.1 μM AP20187 for 8 hr. Cells

were then examined by light microscopy for accumulation of autophagic bodies in the vacuoles (Takeshige *et al.*, 1992). Typical accumulation of autophagic bodies was observed in AP20187 treated cells, but was rarely detected in untreated cells (Fig. 15).

Induction of autophagy was also confirmed by examining the maturation of a vacuolar enzyme, aminopeptidase I (API). In *Saccharomyces cerevisiae*, API is synthesized in a pro-form (proAPI) and delivered from cytoplasm to vacuole via the cytoplasm to vacuole targeting (Cvt) pathway, an autophagy-related pathway (Klionsky *et al.*, 1992; Baba *et al.*, 1997; Scott *et al.*, 1997). During starvation, API is transported to the vacuole via the autophagic pathway. Delivery to the vacuole leads to maturation of API into its active form (mAPI). Δ*apg16* cells expressing $Apg16^{65}$-$2FKBP^{F36V}$ were grown in medium with or without 0.1 μM AP20187 and starved for 3 hr. Lysates were prepared and subjected to immunoblotting using anti-API antibody. While most API was processed to the mature form in wild-type cells (Fig. 16a, *lane 3*), API was scarcely detected in Δ*apg16* cells expressing $Apg16^{65}$-$2FKBP^{F36V}$ (Fig. 16a, *lane 1*). As expected, maturation of API was restored if it is not complete after treatment with AP20187 (Fig. 16a, *lane 2*), in a concentration-dependent manner (Fig. 16b). Taken together, the results of these experiments suggest that formation of the ~350-kDa Apg12-Apg5·Apg16 complex is required for autophagy.

II. Analysis of mammalian autophagy

As describe above, I have shown that the Apg12-Apg5·Apg16 complex is a functional unit for autophagosome formation in yeast. Although the Apg12-Apg5 conjugate is well conserved among all eukaryotes (Mizushima *et al.*, 1998b), no apparent homologue of yeast Apg16 was found in other species by database searching. Dose Apg12-Apg5 conjugate form a protein complex in other eukaryotes? If so, a functional counterpart of Apg16 would exist to closs-link Apg12-Apg5 conjugate. I next studied mammalian Apg12-Apg5 conjugate to answer this question. It would be helpful to understand the general machinery for autophagosome formation.

Identification of Apg16L

First, I examined whether mammalian Apg12-Apg5 conjugate was involved in a large complex like yeast. As most Apg12-Apg5 conjugated mainly recovered in the cytosolic fraction by differential centrifugation analysis in mouse ES cells (Mizushima *et al.*, 2001)(Fig. 17a), S100 fraction of ES cell lysates was subjected to gel filtration analysis using a Superose 6 column. The Apg12-Apg5 conjugated was eluted in a single fraction peak corresponding to ~800 kDa (Fig. 17b), much larger than the yeast Apg12-Apg5·Apg16 complex (Fig. 6). Therefore, mouse Apg12-Apg5 conjugate forms a protein complex as same as yeast with additional protein(s).

Several Apg5-binding proteins had been isolated in our laboratory. These proteins were isolated by co-immunoprecipitaion using anti-GFP antibody on $APG5^{-/-}$ ES cells stably expressing GFP-Apg5 (clone GFP24) (Mizushima *et al.*, 2001). As shown in Fig. 18a, anti-GFP immunoprecipitates from total cell lysates of [^{35}S]-labelled GFP24 cells contained several specific proteins of p63, p71 and p144, in addition to ^{GFP}Apg5 and Apg12-^{GFP}Apg5. These proteins were not present in precipitates from wild-type ES cells expressing GFP alone. These proteins may be additional subunits of the ~800-kDa complex. To identify these proteins, cell lysates prepared from GFP24 ES cells were passed over an anti-GFP antibody-coupled protein A-Sepharose column. Bound proteins were eluted and separated by SDS-PAGE (Fig. 18b). Coomassie stained gel bands corresponding to p63 and p71 were

digested in situ with lysyl-endopeptidase. Mass spectrometric protein identification revealed that both p63 and p71 represent a novel protein, predicted by several expressed sequence tags (AI037166, BI687378, BB620083, AA982950, BE3714456, BB660407, BB839395, BB853783 etc.)(Fig. 19). As this protein shares several features with yeast Apg16 (described below), it was named Apg16L (Apg16-like protein).

Spliced isoforms of Apg16L

Apg16L is expressed ubiquitously in mouse tissues (Fig. 20b). However, the size of Apg16L differed among the tissues and cell lines tested. The liver, kidney, spleen, thymus and testis contained a major form of 63 kDa with a minor form of 71 kDa (Fig. 20b)(data not shown for spleen, thymus and testis). This expression pattern was also observed in ES cells, which is consistent with the results of immunoprecipitation and affinity-purification using anti-GFP antibody (Fig. 18). In contrast, a larger 75-kDa form was the most abundant form in brain, skeletal muscle (Fig. 20b) and heart (data not shown). Both the 63-kDa and 71-kDa proteins were the major forms in HeLa cells. The genomic DNA sequence and the cDNA sequences of the EST database suggested that the Apg16L gene encodes multimeric isoforms. Sequence analysis confirmed that at least three isoforms of Apg16L were generated by alternative splicing events (Fig. 20a). The major cDNA present in liver, designated as Apg16□, lacks all of exons 8 (57 bp) and 9 (48 bp). The minor cDNA present in liver, designated Apg16□, lacks the exon 9. The major cDNA in brain, designated as Apg16□, contains the complete sequences of both exons 8 and 9. Transient transfection of Apg16□ cDNA into HeLa cells increased the levels of p63 (Fig. 20b, lane 7). Therefore, the p63 and p71 proteins affinity-purified from ES cell lysates represented Apg16□ and Apg16□, respectively. The RT-PCR pattern amplifying exons 8 and 9 is shown in Fig. 20c.

Structure and homologues of Apg16L

Apg16L contains a coiled-coil region at the N-terminal region (amino acid 91-190) and seven WD repeats in the C-terminus (outlined in black in Fig. 21a). WD repeats are implicated in protein-protein interactions (Smith *et al.*, 1999). The

peptides encoded by exons 8 and 9, deleted in Apg16L and Apg16L, are located between the coiled-coil region and WD repeat. Putative Apg16L homologues are present in various eukaryotes, but are not present in *Saccharomyces cerevisiae* (Fig. 22a). However, the N-terminal region including the coiled-coil motif (amino acid 106-208) demonstrated a significant homology with yeast Apg16 (amino acid 28-145) (22% identity and 43% similarity)(Fig. 21b). Suggesting from that Apg16L was isolated from the complex containing Apg5, Apg16L has a function similar to yeast Apg16.

Apg16L interacts with Apg5 and Apg16L itself

I next examined whether Apg16L indeed interacts with Apg5. HeLa cells were transiently transfected with FLAG-tagged mouse Apg16L and/or HA-tagged human Apg5. Immunoprecipitation analysis using anti-FLAG or anti-HA antibody revealed that Apg16L and Apg5 were specifically co-precipitated (Fig. 22a). Both Apg12-conjugated and unconjugated Apg5 were immunoprecipitated with anti-FLAG antibody, suggesting that Apg16L interacts directly with Apg5, but not with Apg12. I determined the specific Apg5-binding domain of Apg16L using a yeast two-hybrid assay. The extreme N-terminal region of Apg16L (amino acid 1-79), upstream of the coiled-coil region, is sufficient to interact with Apg5 (Fig. 23). This is consistent with the interaction of yeast Apg16 with yeast Apg5 through the corresponding region (Mizushima *et al.*, 1999). I also observed that the N-terminal region of Apg16L (amino acid 1-276) forms homo-dimer, although I could not determined the sub-region required in greater detail. As yeast Apg16 forms homo-oligomer through its coiled-coil domain, it was speculated that the coiled-coil domain of mouse Apg16L also self-associates. These data also demonstrated that the WD domain is required for neither Apg5-interaction nor homo-oligomerization.

Although I could not detect homo-dimerization of full-length Apg16L by two-hybrid analysis, this self-association was demonstrated by co-immunoprecipitation experiments in wild type ES cells transiently expressing both GFP- and FLAF-tagged Apg16L. When GFP-tagged Apg16L was precipitated with anti-GFP antibody, FLAG-tagged Apg16L was co-precipitated (Fig. 22b) and *vice versa* (data not shown). Apg16L self-interaction did not require Apg5, as similar

results were obtained when using *APG5*$^{-/-}$ ES cells (Mizushima *et al*., 2001). Thus, Apg16L likely forms a homo-oligomer.

Apg12-Apg5 and Apg16L form a ~800-kDa protein complex

Since the interaction between Apg5 and Apg16L was confirmed, I further examined whether Apg16L was contained in the ~800-kDa protein complex with the conjugate. As previously reported, in wild-type ES cells, almost all Apg12-Apg5 conjugated mainly recovered in the cytosolic fraction by differential centrifugation analysis (Mizushima *et al*., 2001)(Fig. 24a). Apg16L was also primarily recovered in S100 fractions of both Apg5$^{+/+}$ and Apg5$^{-/-}$ ES cell homogenates, suggesting that most Apg16L is present in the cytosol (Fig. 24a). Although the presence of physiological concentration of salt in the lysis buffer is considerably important for such differential centrifugation experiments of yeast cell lysates (Fig. 2), the results of mammalian cells was not affected by salt concentration (data not shown)

To determine whether Apg16L is contained in the ~800-kDa complex, gel filtrate analysis was performed. The S100 fraction was subjected to gel filtration analysis using a Superose 6 column and each fraction was immunoblotted with anti-Apg5 and anti-Apg16L antibodies. The Apg12-Apg5 conjugate from multiple tissues and cell lines eluted primarily in fractions corresponding to ~800 kDa, with and occasional minor peak observed at ~400 kDa. This result conflicted with the data obtained using yeast cells, in which Apg12-Apg5 and Apg16 form a ~350-kDa complex. The elution pattern of all three isoform of mouse Apg16L was similar to that of Apg12-Apg5 (Fig. 24b). Co-elution of Apg12-Apg5 conjugate and Apg16L indicated that most of the Apg12-Apg5 conjugate and Apg16L are contained within the ~800-kDa protein complex. All three Apg16L isoforms can be recruited into the complex. Monomeric Apg12-apg5 conjugate and Apg16L were not detected. Formation of the ~800-kDa complex was not affected by nutrient conditions.

In *APG5*$^{-/-}$ ES cells, however, this ~800-kDa complex was not formed. Apg16L was recovered as a single peak in fractions corresponding to ~250 kDa, a size larger than the molecular mass of Apg16L monomer (Fig. 24b). It is unlikely that additional components are contained in the complex, as other stoichiometric subunits were not detected (Fig. 18). The amount of p144 precipitated with Apg5

was minimal enough that it would not contribute to the molecular mass of the complex. Therefore, I assume that the ~250-kDa complex in the APG5$^{-/-}$ ES cells represents a tetrameric Apg16 oligomer.

Apg16L localizes to autophagic isolation membrane

It was reported that a small fraction of the cytosolic Apg12-Apg5 conjugate localizes to pre-autophagosomal membranes, playing an essential role for in the elongation of the membrane. Thus, I examined whether Apg16L is localized to pre-autophagosomal membrane together with Apg12-Apg5. ES cells stably co-expressing combinations of fluorescently tagged Apg5, Apg16L and LC3 were generated. LC3, a mammalian homologue of Apg8, serves as a molecular marker of autophagosomes (Kabeya *et al.*, 2000). Upon the induction of autophagy by the depletion of serum and amino acids, YFP-LC3 associated with both pre-autophagosomal membranes and completely formed autophagosome. As autophagosomes size in ES cells is larger than in other cell lines, LC3 labeling was often identified as a ring-shaped structure even when using conventional fluorescent microscope (Fig. 25a right panel). Apg5 was, however, present only on the pre-autophagosomal membranes enclosing the cytoplasm, not on ring shaped autophagosome (Fig. 25a, middle panel) (Mizushima *et al.*, 2001). The subcellular localization of Apg16L was similar to Apg5. CFP-Apg5 positive isolation membranes clearly co-labeled with YFP-Apg16L (Fig. 25b). While the Apg16L-labeled structure was positive for LC3, Apg16L never co-localized with the LC3-positive ring-shaped structures (Fig. 25c). These data suggests that the Apg12-Apg5 conjugate and Apg16L localized to the pre-autophagosomal membrane as a complex.

Screening of Apg16L binding protein

As shown in Fig. 18, Apg12, Apg5 and Apg16L are the main components of the ~800-kDa complex. Although WD domain is known to be a scaffold for protein interaction, it was not required for either the interaction with Apg5 or homo-oligomerization (Fig. 23). The WD domain of Apg16L indicates the involvement of other proteins. Thus, I performed two-hybrid screens using Apg16L as bait to

identify Apg16L-interacting protein. The bait plasmid (pGBD-APG16L) and prey plasmid containing mouse embryonic cDNA library fused to the GAL4 activating domain were sequentially transformed in L40 yeast strain. Screening was done several times until enough number of transformants were obtained. As a result, 5 positive clones were obtained, which coded for total of 4 different proteins (Fig. 26). Sequencing studies revealed that these proteins were antinin-2, T6BP and PurB. Actinin-2 is an actin cross-linking protein, T6BP is TRAF binding protein which inhibits apoptosis and PurB is involved in the initiation of DNA replication. I am now evaluating these interactions in mammalian cells.

Discussion

Endogenous Apg12-Apg5 conjugates present mainly in the cytosol.

It was reported that HA-tagged Apg12 was conjugated to Apg5 less than half of it in yeast (Mizushima *et al*., 1998a). However, I showed most of endogenous Apg12 is found attached to Apg5 in both yeast and mammalian cells (Fig. 1and Fig. 23a). It is conceivable that plasmid-derived expression of HA-Apg12 affects the conjugation efficiency. HA-tagging may also affect the subcellular distribution determined from differential centrifugation experiments. Previous reports showed that most HA-tagged Apg12-Apg5 was pelletable (Mizushima *et al*., 1999), even when lysis buffer containing salt was used (George *et al*., 2000). In contrast, as shown in Fig. 3, the endogenous Apg12-Apg5 conjugate was recovered primarily in the cytosolic fraction. The same result was obtained in mammalian cells. Combined with our recent morphological studies demonstrating that most Apg12-Apg5 is found in the cytoplasm (Suzuki *et al*., 2001Mizushima *et al*., 2001), I concluded that cytosol is the primary localization of endogenous Apg12-Apg5. Under the present conditions, a small portion of Apg12-Apg5 was still observed in the pellet fractions (Fig. 3). However, its amount was not changed during nitrogen starvation or in yeast cells disrupted *apg*6, in which the pre-autophagosomal structures were not formed (Mizushima *et al*., 2001; Suzuki *et al*., 2001). Therefore, it is dubious that the conjugate in the pellet fractions represents any real physiological localization.

Apg12-Apg5 forms the protein complex with Apg16 (L).

Gel filtration analysis showed that almost all yeast Apg12-Apg5 conjugate and Apg16 formed ~350-kDa complex. Similarly, almost Apg12-Apg5 conjugate and Apg16L were contained in a ~800-kDa complex in mammalian cells. This is not simply because each monomer is unstable; free Apg12-Apg5 conjugate, Apg16 and Apg16L were easily detected in yeast of Δ*apg16*, Δ*apg5* cells and Apg5$^{-/-}$ ES cells respectively, neither of which contain the complexes (Fig. 7 and Fig. 23b). Judging from that the Apg12-Apg5・Apg16 (L) complex exists stably irrespective of autophagy-induction, formation of the complex would not be a trigger of autophagy.

From purification analysis, it is unlikely that other molecules participate in the formation of the Apg12-Apg5·Apg16 (L) complex in both yeast and mammalian cells. Considering the molecular mass of Ap12, Apg5 and Apg16 (MW=21, 33, and 17 kDa, respectively), it is most likely that the yeast ~350-kDa complex includes four sets of Apg12-Apg5·Apg16. The mammalian complex is much larger than that of yeast. The ~800-kDa complex was suggested to include eight sets of Apg12-Apg5·Apg16L (MW=15, 32, and 66 kDa, respectively), while the ~400-kDa minor complex contains four sets (Fig. 23b). If so, the minor ~400-kDa complex may contain equivalent components to the yeast complex.

Oligomerization of yeast Apg16.

In yeast cells, I showed successfully that formation of the ~350-kDa complex is mediated by Apg16 homo-oligomer using the regulated oligomerization system. Although $Apg16^{65}$-$2FKBP^{F36V}$ and Apg12-Apg5 were clearly shifted to ~400 kDa by AP20187 treatment, it was intriguing that these proteins were detected at the fraction corresponding to ~200 kDa in the absence of AP20187. Since $2FKBP^{F36V}$ was inserted immediately after the beginning of the coiled-coil region, the remaining coiled-coil region of Apg16 might mediate formation of dimeric Apg12-Apg5·$Apg16^{65}$-$2FKBP^{F36V}$ complex. If that is the case, it was conceivable that this system regulates tetramer formation by cross-linking the dimeric $Apg16^{65}$-$2FKBP^{F36V}$. I demonstrated that the ~400-kDa Apg12-Apg5·$Apg16^{65}$-$2FKBP^{F36V}$ complex formed by such a manner was functional, suggesting that the wild-type ~350-kDa complex might be also formed by dimer-dimer association. In general, tetramer formation mediated by dimer-dimer contact is possible as observed in the cases of EPS15 (Cupers *et al.*, 1997), F1-ATPase inhibitor protein, IF1 (Cabezon *et al.*, 2000) and Mnt repressor (Berggrun and Sauer, 2001), although four-stranded coiled-coils have been reported (Lupas, 1996). I also tried to test whether Apg16 inserted with a single copy of $FKBP^{F36V}$ domain at the same site was able to function. However, the resulting $Apg16^{65}$-$1FKBP^{F36V}$ was still functional in absence of AP20187, probably due to insufficient interference of the tetramer formation, and thus could not be evaluated (data not shown).

The regulated oligomerization system used in this study is based on

interaction between FK506 and FKBP. Another natural ligand of FKBP is rapamycin, which is known to induce autophagy (Noda *et al.*, 1995). The rapamycin-FKBP complex inhibits Tor kinase, which plays a role in nutrient sensing, thus inducing autophagy (Noda and Ohsumi, 1998; Schmelzle and Hall, 2000; Raught *et al.*, 2001). Therefore, I tested AP20187 to make sure it did not possess a rapamycin-like activity that could affect our results. I confirmed that, in contract to rapamycin, AP20187 itself did not induce autophagy (data not shown). The possibility that AP20187 could induce autophagy through the Tor-mediated pathway was also rejected, because AP20187 and nitrogen starvation had such strong additive effects on autophagy and API maturation (Fig. 16). In this experiment, the $Apg16^{65}$-$2FKBP^{F36V}$ fusion construct allowed for ligand-dependent recovery of the formation of the Apg12-Apg5·Apg16 complex and autophagic activity, suggesting that the Apg12-Apg5 conjugate would not function unless cross-linked by Apg16. On the other hand, Δ*apg16* cells expressing $Apg16^{118}$-$2FKBP^{F36V}$ were defective in autophagy, even though the ~400-kDa complex was present (data not shown). This may indicate that the extreme C-terminal region of Apg16 plays a role in something other than oligomerization. In mammalian cells, considering the structure, protein interaction and localization of Apg16L which is related to the yeast Apg16, formation of the ~800-kDa complex would also depend on Apg16L-oligomerization and requires for autophagy.

Mammalian Apg16L has WD repeat domain.

Although Apg12-Apg5 conjugate was well conserved in yeast and mammalian cells, there are several dissimilar points between yeast Apg16 and mouse Apg16L. The most striking difference is the presence of the WD repeats in mouse Apg16L. This motif, first identified in the β-subunits of trimeric G proteins, forms a β-propeller structure, which creates a stable platform for simultaneous interactions with multiple proteins (Smith *et al.*, 1999). This symmetrical structure usually consists of at least four, typically seven repeats. As the WD domain of Apg16L is not involved in either the interaction with Apg5 or homo-oligomerization, it is likely that yet unknown protein(s) interact with the WD domain. Purification of the ~800-kDa complex, however, demonstrated that Apg12, Apg5 and Apg16L are the main

components. Therefore, the putative WD domain-binding protein may interact with only a small population of the total Apg12-Apg5·Apg16L complex. This protein may promote membrane association of the complex. One attractive idea is that this protein may be a receptor for the Apg12-Apg5·Apg16L complex on the isolation membrane. p144 remains a good candidate; I am now attempting both its purification and identification. It may also be possible that WD-binding protein was involved in other functions not membrane targeting, because yeast Apg12-Apg5·Apg16 complex could target to PAS without WD-repeats domain. The WD domain might function with α-actinin, which was raised from two-hybrid screens. α-actinin is known to cross-link actin filaments into a bundle. As the involvement of actin in mammalian autophagosome formation had been suggested (Aplin *et al.*, 1992; Blommaart *et al.*, 1997), α-actinin might link autophagy system with cytoskeleton. Several proteins which have both WD domain and coiled-coil motif were reported. For example, miosyn heavy chain kinase A (MHCK A) contains an amino-terminal coiled-coil domain, a central catalytic domain, and a carboxyl-terminal domain. MHCK A forms a oligomer through coiled-coil motif and targets a substrate by direct binding WD domain to a substrate (Kolman *et al.*, 2001). Therefore, WD domain of Apg16L would play some role, even though I could not confirm whether WD domain of Apg16L was actually functional.

Multiple homologues of Apg16L in various higher eukaryotes have WD repeats at the C-terminal region except *Saccharomyces cerevisiae* and *Pichia pastoris* (Fig. 21 and Y.Sakai, personal communication). Higher eukaryotic Apg16L may contain a WD domain because the putative binding partners of this domain may mediate additional autophagic machinery specific to higher eukaryotes. The several differences in autophagosome formation between yeast and mammalian cells may be controlled by this WD repeat-containing region. Yeast autophagosomes are generated from a single pre-autophagosomal structure in the perivacuolar region, whereas several autophagosomes can be generated at the same time from multiple sites in mammalian cells. Size variation of autophagosomes is also much larger in mammalian cells than in yeast cells. Therefore, higher eukaryotes may have developed extra machinery creating these inherent differences from yeast in autophagosome formation. In addition, a yet unidentified WD repeat protein

corresponding to the C-terminal half of Apg16L may function together with Apg16 in yeast. Genome sequencing revealed that yeast possesses at least 60 WD repeat proteins, many of unknown function. It is also possible that a short segment at the extreme C-terminal region (downstream of the coiled-coil region) of yeast Apg16 could exert a function corresponding to that of the Apg16L WD domain.

Apg16L is expressed in different isoform patterns depending on the mouse tissue. I identified three isoforms produced by alternative splicing. I could not discern any differences among these isoforms in complex formation; each can be incorporated into the ~800-kDa complex. The possibility remains, however, that the Apg16L isoforms differ in additional functions.

The function of Apg12-Apg5・Apg16 (L) complex through autophagy.

It was reported that the Apg12-Apg5 conjugate functions in elongation step of pre-autophagosomal membrane, but the exact molecular mechanism is unknown. Recent morphological studies showed that Apg12-Apg5 conjugate is localized to PAS or pre-autophagosomal membrane in both yeast and mammalian cells. Yeast Apg16 is also observed in PAS. Considering with my data, that Apg12-Apg5・Apg16(L) complex would be formed in cytosol and then a portion of it targets to PAS or pre-autophagosomal membrane, and functioned on it (Fig. 27). It was shown in Δ*apg16* yeast cells that membrane targeting of Apg5 requires Apg16 (Suzuki *et al.*, 2001). One role of Apg16 might be recruitment of the Apg12-Apg5 conjugate to PAS. However, membrane targeting of Apg16 also requires Apg5, which was determined using Δ*apg5* yeast cells and APG5$^{-/-}$ ES cells. In yeast, Apg5 and Apg16 could form a complex without Apg12, and Apg5-Apg16 is targeted to PAS. Therefore, the interaction between Apg5 and Agp16 is essential and sufficient for the binding of the complex to the pre-autophagosomal membrane. Thus, the covalent modification of Apg5 with Apg12 is not required for membrane targeting of Apg5 and Apg16 but is essential for membrane elongation. Using oligomerization system, I demonstrated that oligomerization of Apg16 is essential for autophagy, but I could not conclude whether Apg16 oligomerization is essential for Apg12-Apg5 recruitment.

Considering that Apg12-Apg5 conjugate preferentially localizes to the

outer side of the elongating autophagic isolation membrane in mammalian cells (Mizushima *et al*., 2001), there is the possibility that Apg12-Apg5 functions like coat proteins required for conventional membrane budding. Intracellular trafficking of proteins along the secretory pathway is mediated by transport vesicles, which are generated by the action of coat proteins. To make the vesicles, cytosolic coat proteins assemble on a donor membrane and deform it into a bud. After vesicle budding, coat proteins dissociate from the vesicle membrane. The behavior of Apg12-Apg5 conjugates is similar to that of coat proteins. Another possibility is that the Apg12-Apg5 conjugate might catalyze the modification of Apg8/LC3 or recruit of Apg8/LC3 to membrane where Apg8 is modified, because modification and localization of Apg8 depends on Apg12-Apg5 conjugate. Although interaction between Apg8 and Apg12-Apg5 conjugate was reported, cytosolic Apg8, Apg3 and Apg12-Apg5 were not co-eluted in my gel filtrate analysis. It was suggested that very small portion of these proteins might be interacting in the cytosol or they were co-localized on some membrane structures. It was interesting that Apg3 eluted in fractions larger than expected molecular size of it. Apg3 might be as a complex in the cytosol with some proteins, for example, Apg4 or Apg7, which are the Apg8 system proteins. To elucidate the relationship between Apg12 and Apg8 system would be a great help to understand the mechanism of autophagosome formation.

In this study, I demonstrated the similarity between yeast and mammalian autophagy system. In both cells, the Apg12-Apg5 conjugate functions as a protein complex with Apg16 (L). Multiple homologues of Apg16L exist in higher eukaryotes, suggesting that the autophagic machinery is well conserved.
I also demonstrated the differences of the Apg12-Apg5･Apg16 complex between yeast and mammalian cells. Apg16L of various eukaryotes have WD domain except *Saccharomyces cerevisiae* and *Pichia pastoris*. Identification of the proteins which binds to WD domain of Apg16L would provide variable information to understand the function of Apg12-Apg5･Apg16L complex. It would also be a help to understand the extra machinery specific to higher eukaryotes if WD domain was involved in it. Further studies aimed at investigating these problems will improve our understanding of the molecular mechanisms of autophagosome formation.

I. Analysis of yeast autophagy

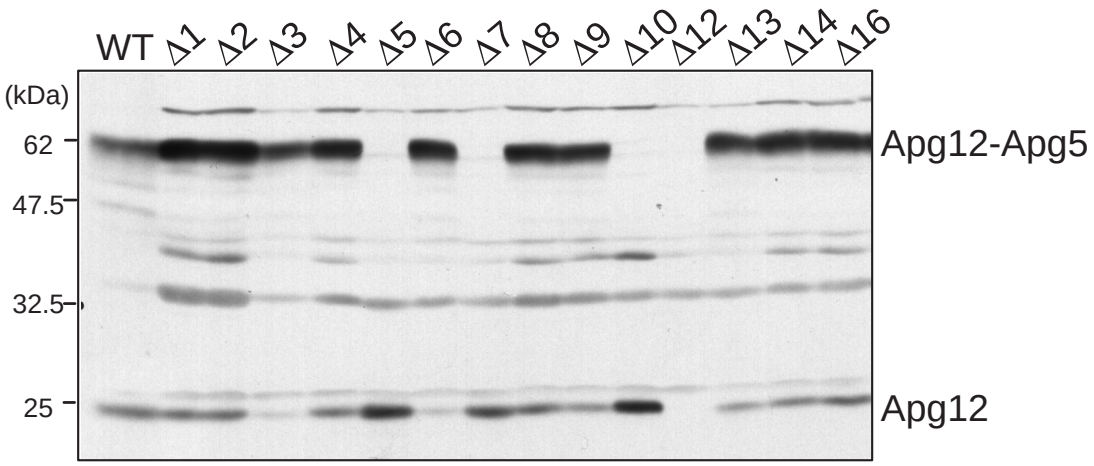

Fig. 1 Expression of endogenous Apg12-Apg5 conjugate. Lysates from wild-type cell (SEY6210) and each *apg* disruptant were immunoblotted using anti-Apg12 antibody. Positions of Apg12-Apg5 conjugate and unconjugated Apg12 are indicated.

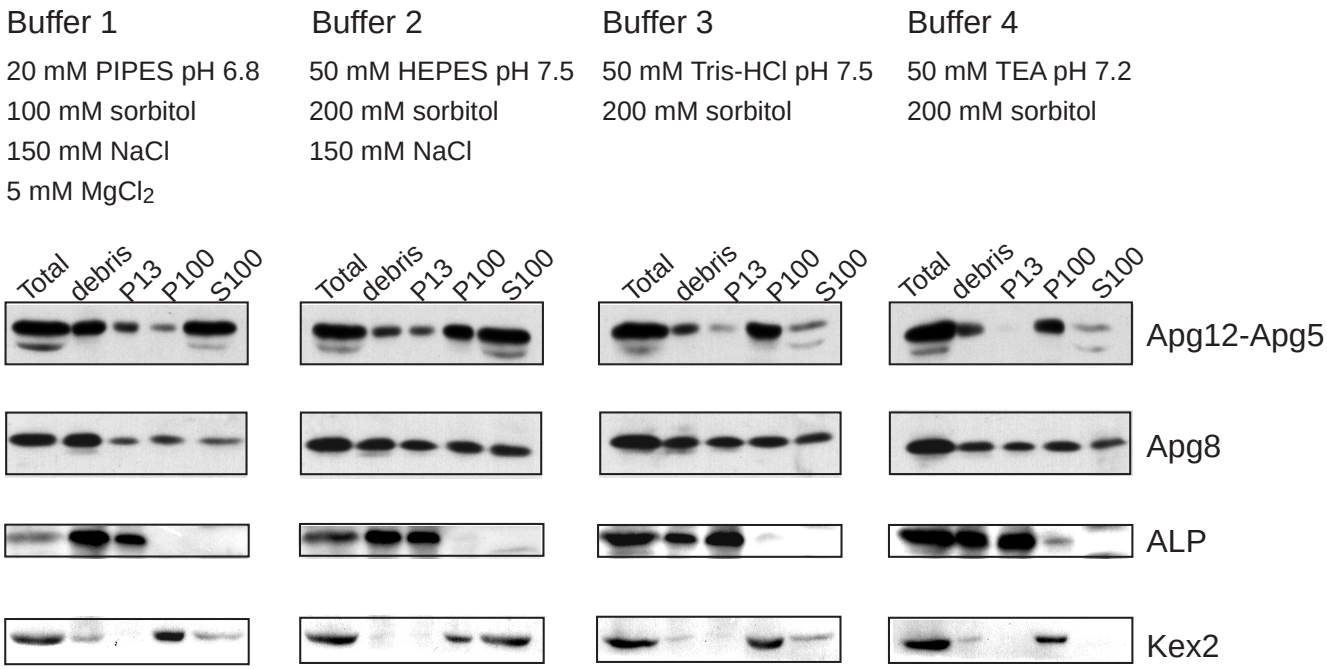

Fig. 2 Subcellular distribution of endogenous Apg12-Apg5 in different buffers. Spheroplasts generated from wild-type cells were homogenized in each type of lysis buffer (buffer 1- buffer 4). After removing the debris, total lysates (T) were subjected to low-speed centrifugation at 13 k x *g* for 20 min to generate a pellet fraction (P13). The resulting supernatant was separated into pellet (P100) and supernatant (S100) fractions by centrifugation at 100 k x *g* for 1 hr. Each fraction was subjected to immunoblotting using anti-Apg12 and anti-Apg8 antibodies. Distribution of organelle marker proteins were examined using anti-ALP and anti-Kex2 antibodies. ALP; vacuolar marker recovered in P13. Kex2; golgi marker recovered in P100.

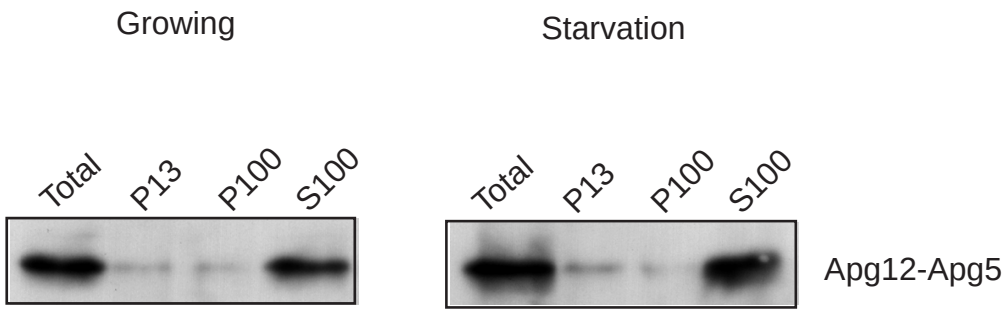

Fig. 3 Subcellular distribution of endogenous Apg12-Apg5 conjugate under the starvation condition in wild-type cells. Lysates were prepared from wild-type cells which were growing in YPD or starved with SD (-N) for 3 hr, and fractionated as discribed in Fig. 2. Each fraction was subjected to immunoblotting using anti-Apg12 antibody.

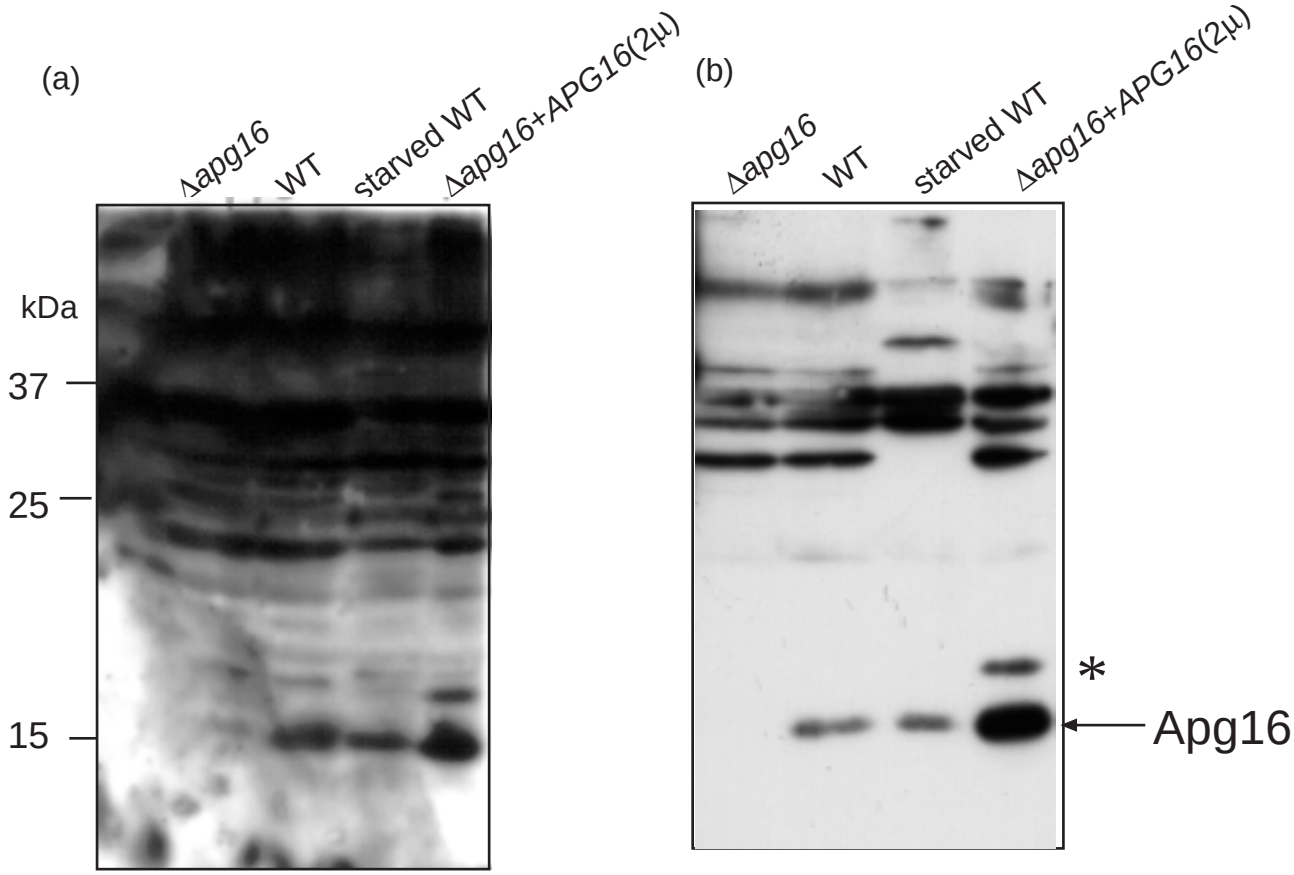

Fig. 4 Affinity-purification of anti-Apg16 antibody. Expression of Apg16 in Δ*apg*16, WT, starved WT, Δ*apg16* cells over-expressing Apg16 by a 2μ plasmid were examined by immunoblotting using anti- Apg16 antibody before(a) or after (b) affinity purification. Positions of Apg16 and its uncharacterized modified form (*) are indicated.

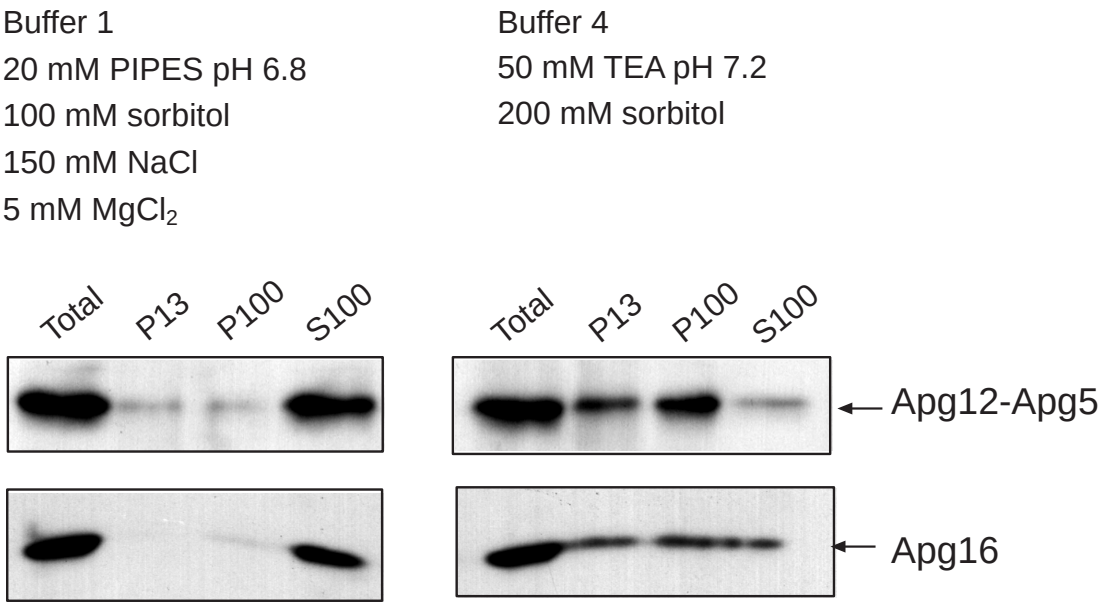

Fig. 5 Subcellular distribution of endongenous Apg16. Spheroplasts generated from wild-type cells were lysed in buffer 1 or buffer 4 used in Fig. 2. Following subcellular fractionation, each fraction was subjected to immunoblotting using anti-Apg16 and anti-Apg12 antibodies. Positions of Apg16 and Apg12-Apg5 conjugte are indicated.

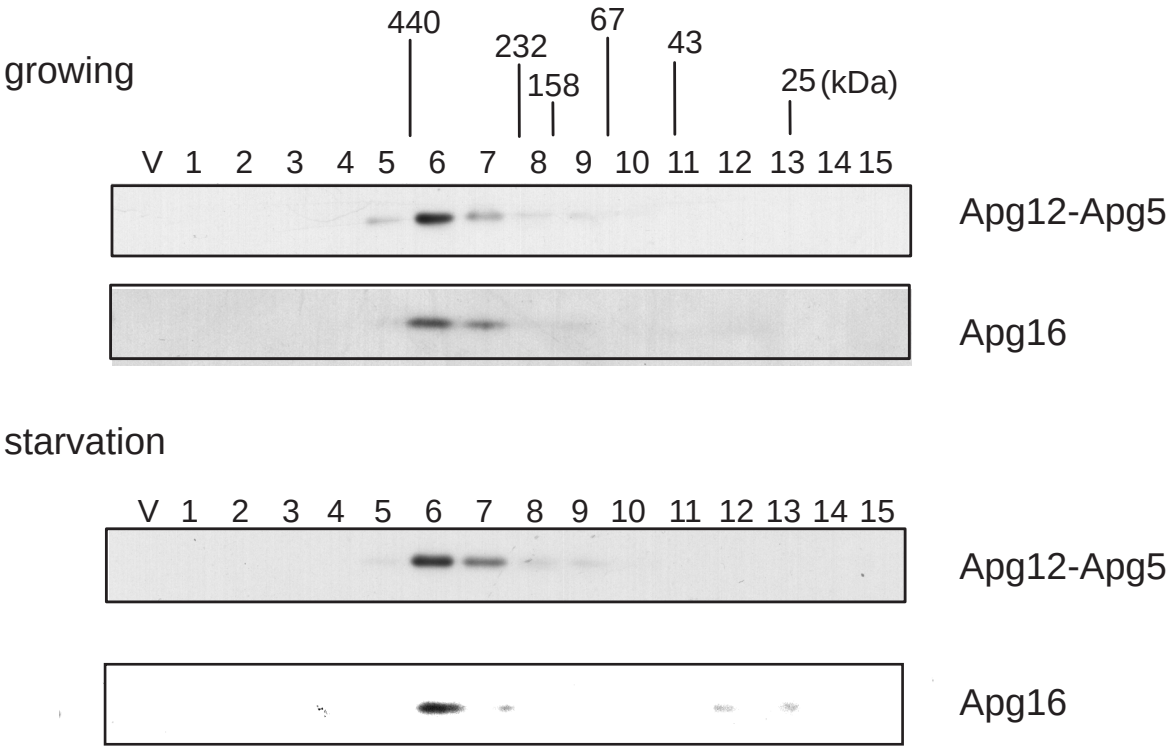

Fig. 6 Apg12-Apg5 and Apg16 form a ~350-kDa complex in the cytosol. The S100 fractions were prepared from wild-type cells which were growing or starved for 3 hr with SD (-N) medium, and separated by size exclusion chromatography on a Superdex 200 column. Each fraction was subjected to immunoblotting using anti-Apg12 and anti-Apg16 antibodies. Positions of molecular mass standards (in kDa) are shown. V, void fraction.

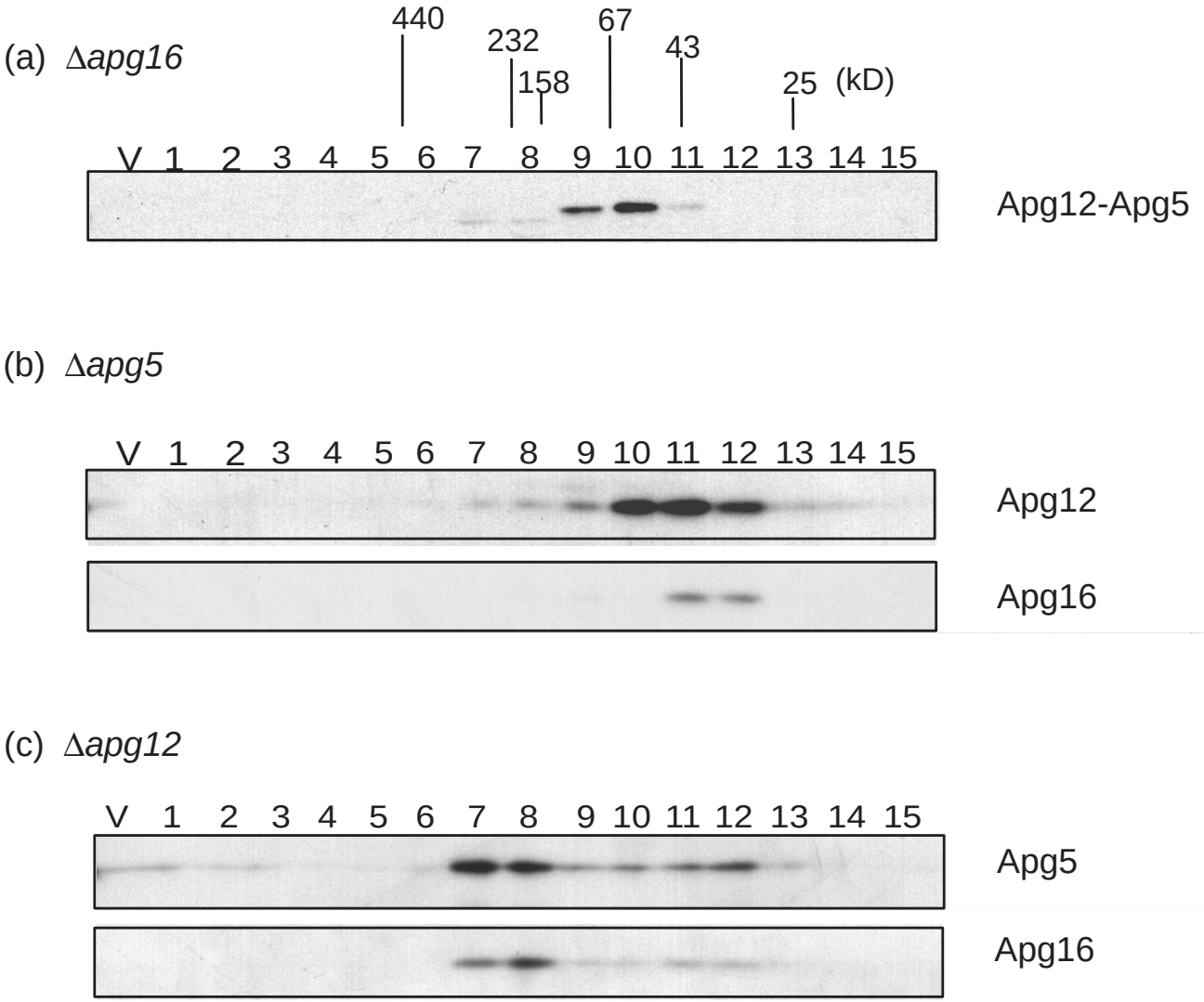

Fig. 7 The ~350-kDa complex is not formed in Δ*apg16*, Δ*apg5* and Δ*apg12* cells.
The S100 fractions from Δ*apg16* (a), Δ*apg5* (b) and Δ*apg12 (*c) cells were subjected to gel filtration analysis using a Superdex 200 column. Each fraction was subjected to immunoblot analysis using anti-Apg12, anti-Apg5 and anti-Apg16 antibodies.

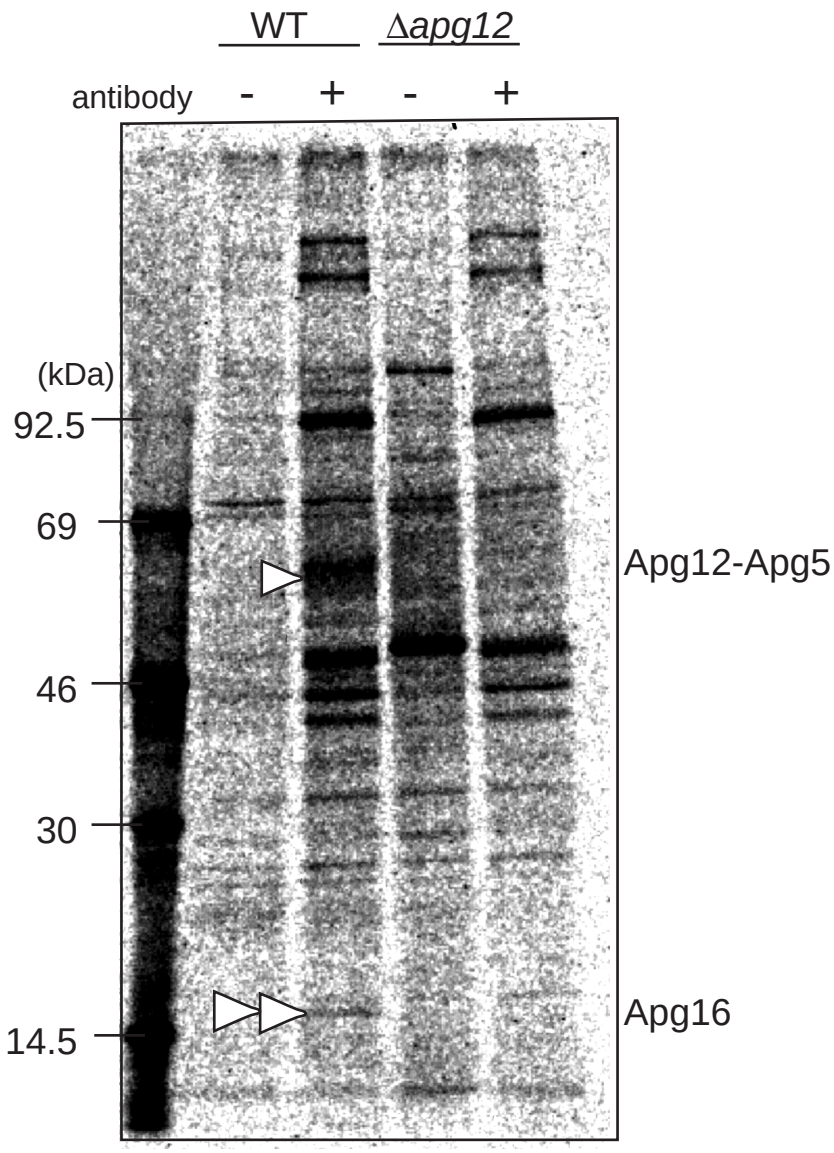

Fig. 8 Immunoprecipitaion of the ~350-kDa complex. Wild-type and Δ*apg12* cells were grown in SD medium supplemented with amino acids without methionine at 30 °C overnight. Cells were labeled with [^{35}S] methionine, and their lysates were prepared. After solubilization with Triton X-100, the lysates were subjected to imuunoprecipation with anti-Apg12 antibody. Immunoprecipitates were separated by SDS-PAGE and visualized by autoradiography using BAS2000.

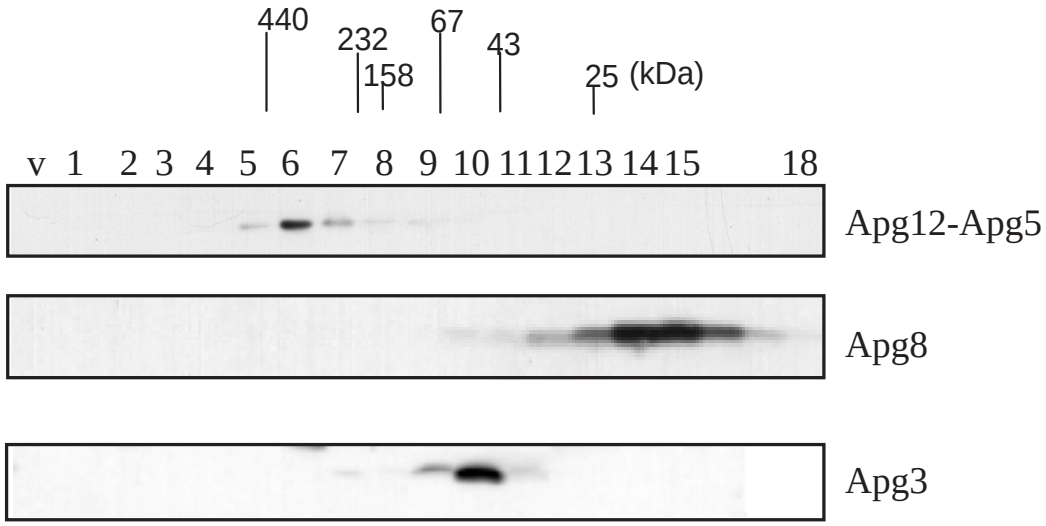

Fig. 9 Co-localization analyses of cytosolic Apg12-Apg5, Apg8 and Apg3.
The S100 fractions were prepared from growing wild-type cells, and separated by size exclusion chromatography on a Superdex 200 column. Each fraction was subjected to immunoblotting using anti-Apg12, anti-Apg8 and anti-Apg3 antibodies. Positions of molecular mass standards (in kDa) are shown. V, void fraction.

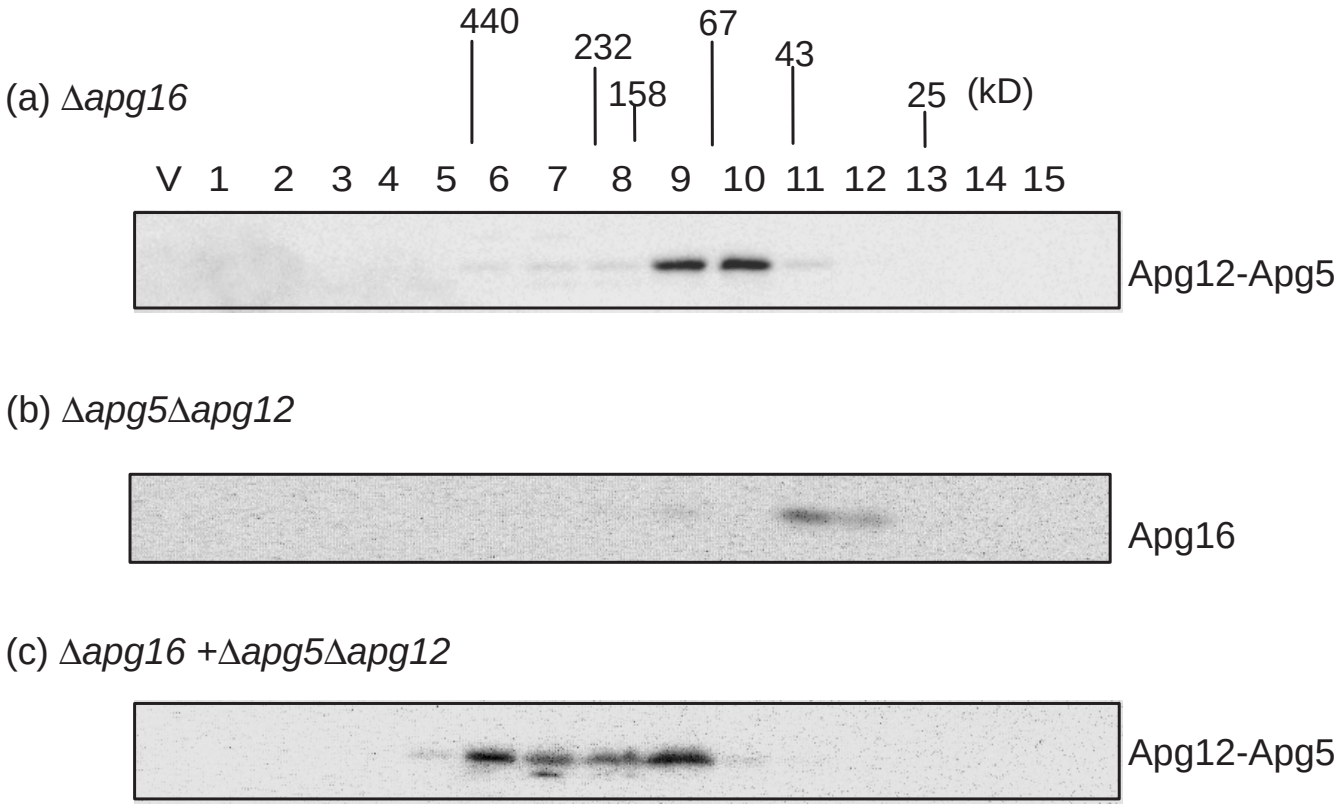

Fig. 10 The ~350-kDa complex is formed *in vitro* using Δ*apg16* and Δ*apg5*Δ*apg12* cell lysates. The S100 fractions from Δ*apg16* cells (a) and Δ*apg5*Δ*apg12* cells over expressing Apg16 from a 2μ plasmid (b) were prepared. Equal volume of these two cell lysates were mixed, incubated at 4°C overnight and subjected to gel filtration analysis using a Superdex 200 column. Each fraction was analyzed by immunoblotting using anti-Apg12 (a, c) and anti-Apg16 antibodies (b).

(a) Structure of Apg16.

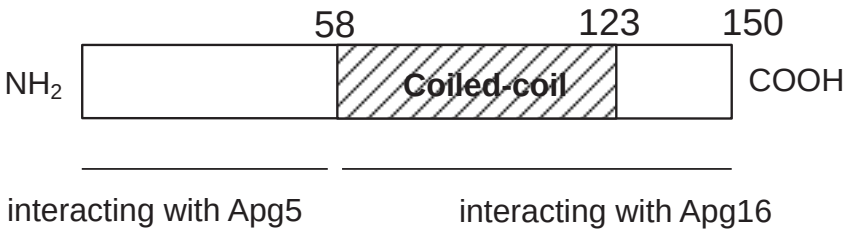

(b) Hypothesis of the formation of Apg12-Apg5*Apg16 complex.

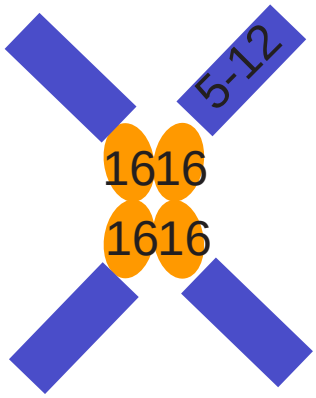

Fig. 11 Apg16 is a coiled-coil protien. (a) Apg16 consists of 150 amino acids and contains coiled-coil motif at it C-terminal half. Apg16 interacts with Apg5 at N-terimnal region and with Apg16 itself at C-terminal half. (b) A hypothesis of the formation of Apg12-Apg5•Apg16 complex. Since Apg16 forms an oligomer and associates with the Apg12-Apg5 conjugate, it would function as a linker of the Apg12-Apg5 conjugate to form the ~350-kDa complex.

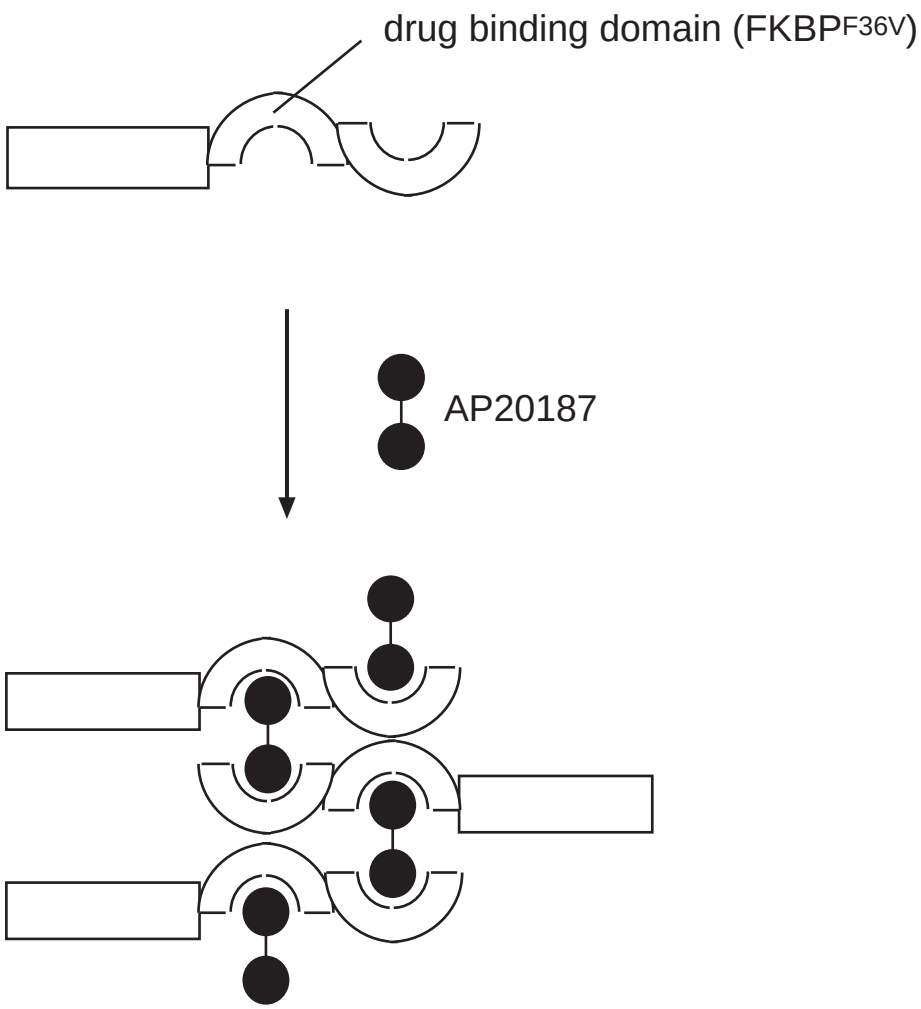

Fig. 12 Scheme of the regulated oligomerization system. A bivalent drug AP20187, which is created by chemically linking two FK506 derivatives, is able to cross-link the FKBP^{F36V} domain. Thus, addition of AP20187 to the cells expressing FKBP^{F36V}-fused proteins will result in the genelation of oligomer.

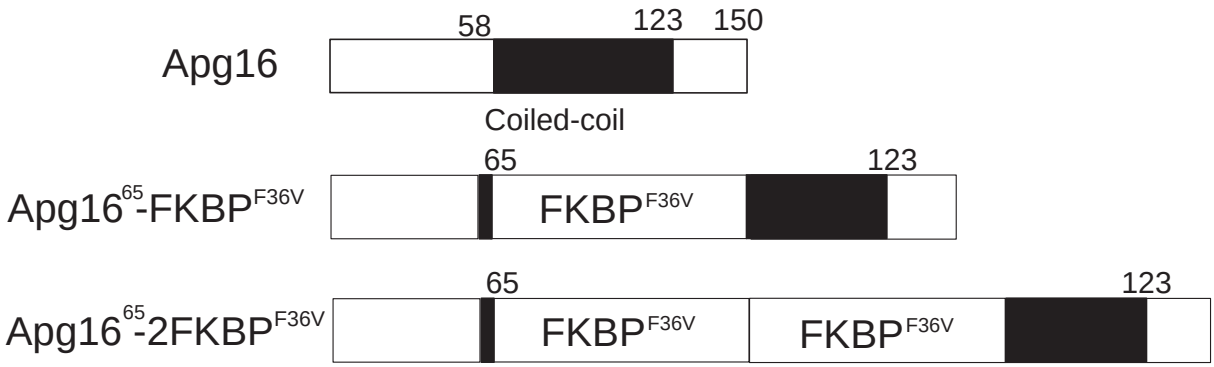

Fig. 13 Schematic diagrames of Apg16-FKBP^{F36V} fusion proteins.
Black boxes represent the coiled-coil region. One or two copies of the FKBP^{F36V} domain were inserted immediately after the beginning of the coiled-coil motif of Apg16.

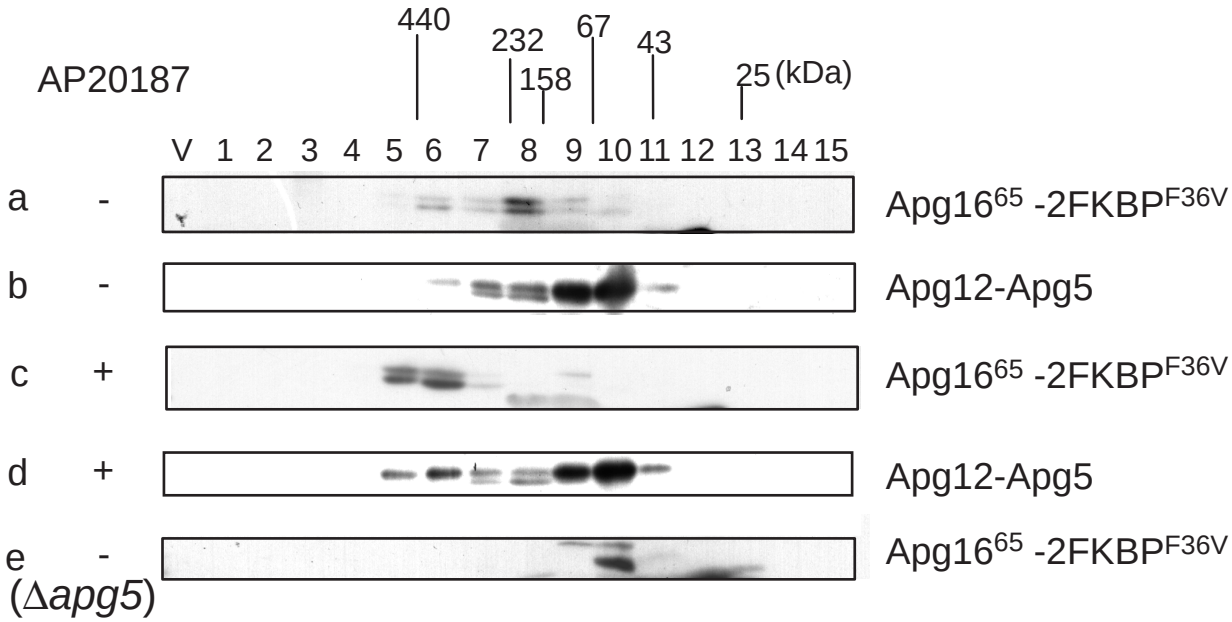

Fig. 14 Regulation of Apg16 oligomerization by synthetic dimerizer AP20187. AP20187 is able to induce oligomerization of Apg16^{65}-2FKBP^{F36V}. Δ*apg16* (*panels a-d*) or Δ*apg5*Δ*apg16* (*panel e*) cells expressing Apg16^{65}-2FKBP^{F36V} fusion protein were incubated with (*panels c and d*) or without (*panels a, b* and *e*) 0.1 μM AP20187 overnight. Lysates were prepared and subjected to gel filtration analysis. Each fraction was subjected to immunoblotting using anti-Apg16 (*panels a, c* and *e*) or anti-Apg12 antibody (*panels b and d*).

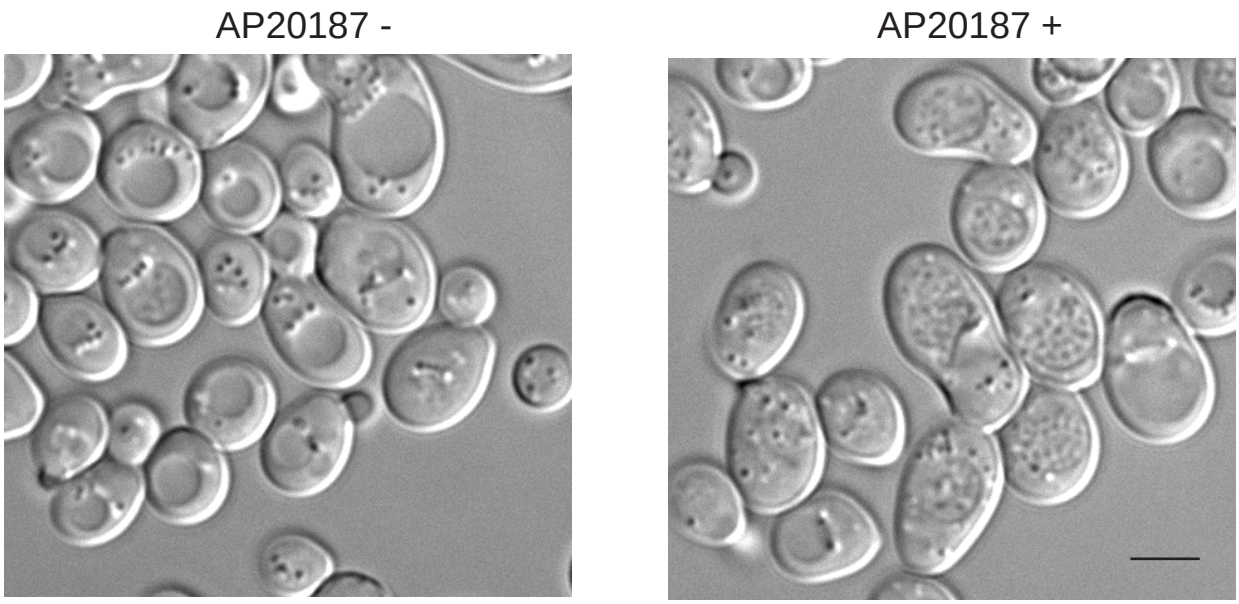

Fig. 15 Accumulation of autophagic bodies is induced by AP20187-dependent Apg16 oligomerization. Δ*apg16* cells expressing the Apg16^{65}-2FKBP^{F36V} fusion protein were grown in nutrient medium with or without AP20187 overnight. Cells were then incubated in SD (-N) containing 1 mM PMSF for 8 hr and observed by light microscopy. Bar: 5 μm.

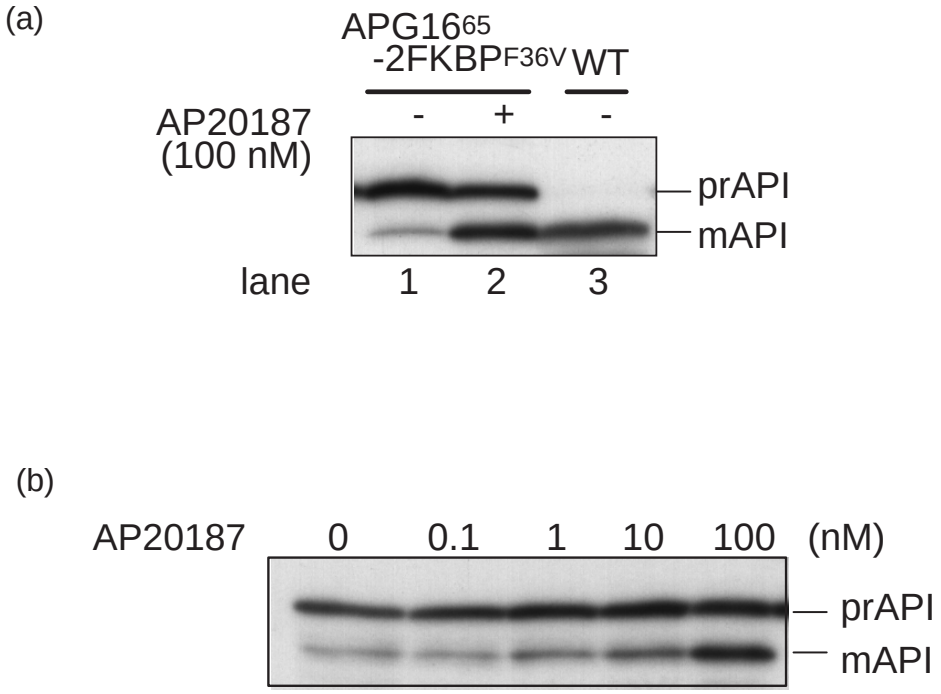

Fig. 16 API-maturation is recoverd by AP20187-dependent Apg16 oligomerization. (a) After treatment with (*lane 2*) or without (*lanes 1* and *3*) 0.1 μM AP20187, Δ*apg16* cells expressing Apg16^{65}-2FKBP^{F36V} (*lanes 1* and *2*) or wild-type cells (*lane 3*) were incubated in SD (-N) for 3 hr. Total lysates were prepared and subjected to immunoblotting using anti-API antibody.
(b) Δ*apg16* cells expressing Apg16^{65}-2FKBP^{F36V} were incubated with the indicated concentration of AP20187 and analyzed as described in (a).

II. Analysis of mammalian autophagy

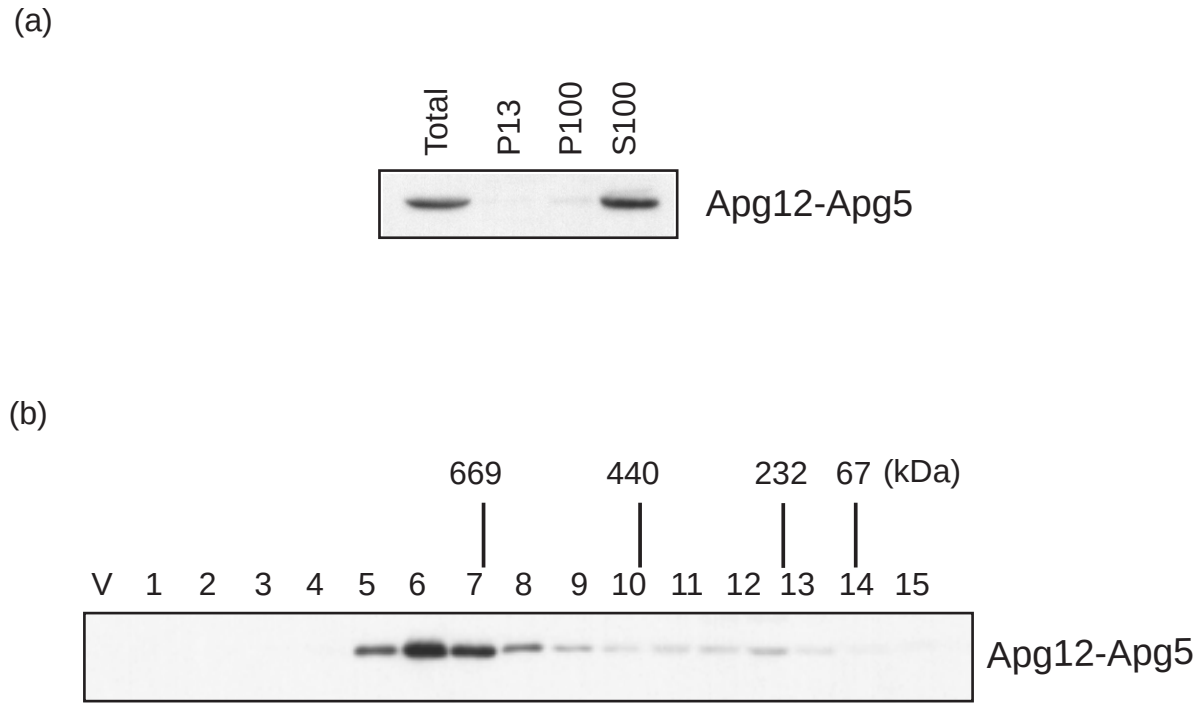

Fig. 17 The Apg12-Apg5 conjugate forms a ~800-kDa protein complex in the cytosol.

(a) Homogenates of mouse liver (Total) were fractionated into an initial pellet (P13) and a subsequencet pellet (P100) and supernatant (S100) fractions by differential centrifugateion. These fractions were analysed by immunoblotting using antibody against Apg5. (b) S100 fractions of mouse liver homogenates were separated by size exclusion choromatography on a Superrose 6 column. Each fraction was subjected to immunoblotting using anti-Apg5 antibody. Positions of the molecular mass standards (in kDa) are shown. V, void fraction.

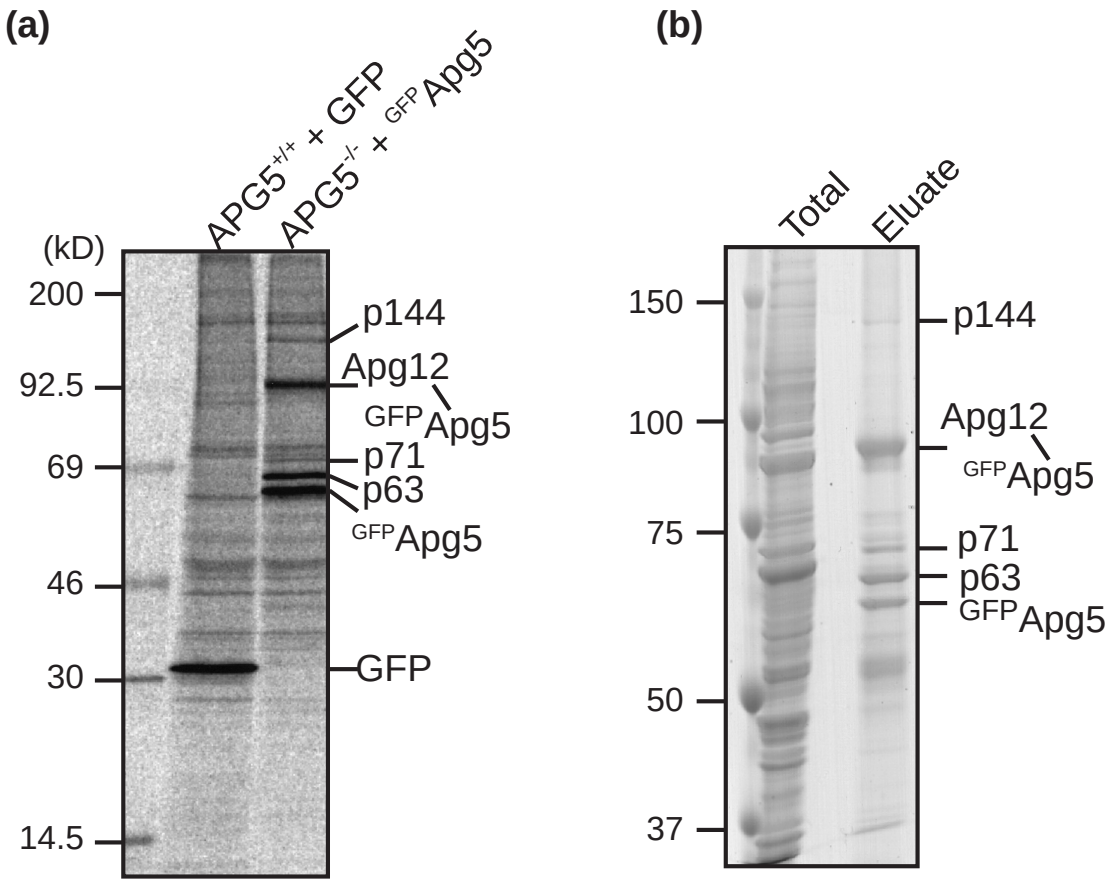

Fig. 18 Identification of proteins interacting with Apg5 in mouse ES cells.
(a) Wild-type ES cells stably expressing GFP and *APG5*$^{-/-}$ ES cells stably expressing GFP-Apg5 (GFP24) were labeled with [^{35}S]methionine/cysteine for two hours. Following immunoprecipitation with anti-GFP antibody from cell lysates, the immunoprecipitates were analyzed by SDS-PAGE and a bioimage analyzer. (b) Total cell lysates were prepared from GFP24 cells and subjected to affinity purification using an anti-GFP antibody-coupled protein A-Sepharose bead column. Following elution, bound proteins were separated by SDS-PAGE and stained with Coomassie Brilliant Blue.

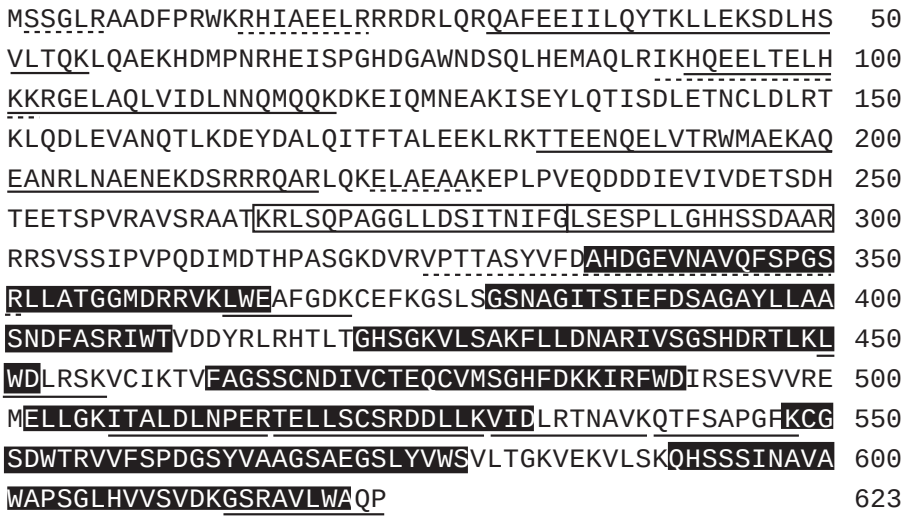

Fig. 19 Amino acid sequence of Apg16L. Underlined and dotted-underlined residues correspond to peptide sequences obtained by mass spectrometry analysis of p63 and p71, respectively. Boxes indicated the peptides encoded by exons 8 and 9. Sequences outlined in black are WD repeats.

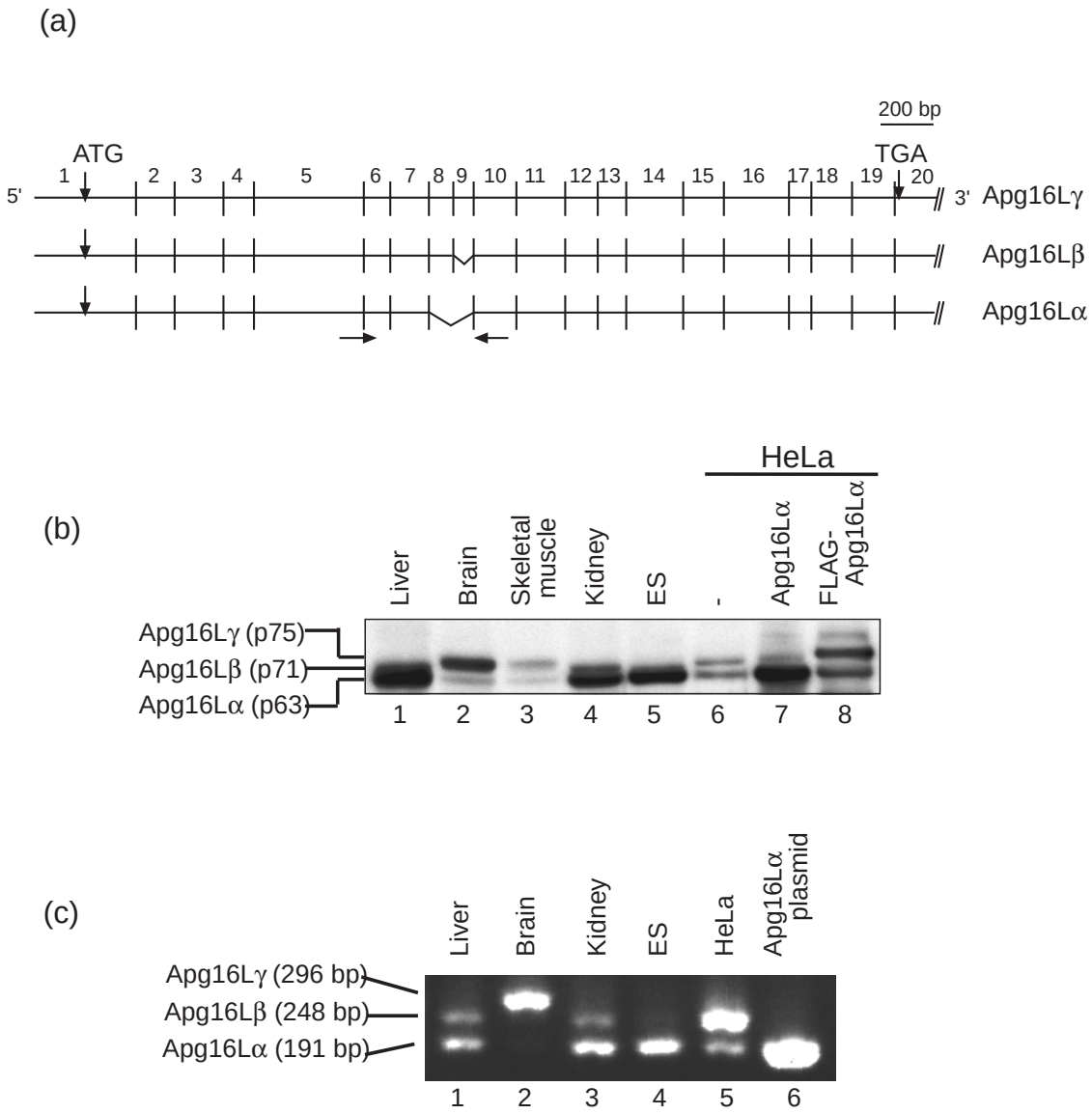

Fig. 20 Structure, splicing isoforms and espression of Apg16L. (a) Alternative splicing of Apg16L mRNA.The 20 exons are indicated by numbers above the line representing Apg16Lγ. Alternatively spliced exons in Apg16Lα and Apg16Lβ are indicated as brokedn lines. (b) Expression of Apg16L in tissues and cell lines. Tissue homogenates were prepared from mouse liver, brain, ther gastrocnemius musc and kidney. These were subjected to immunoblotting using anti-Apg16L antibody. Total cell lysates were also prepared from ES cells and Hela cells transiently transfected with either vector alone, Apg16Lα or FLAG-tagged Apg16Lα. Each lysate was subjected to western blotting using anti Apg16L antibody. The mobility of the three isoforms is indicated. (c) RT-PCR analysis of Apg16L mRNA. Total RNA was isolated from mouse tissues and cultured-cells, and then reverse-transcribed into cDNA. A fragment of the Apg16L cDNA corresponding to exons 6-10 was amplified using the primers indicated by arrows in (a).

(a)

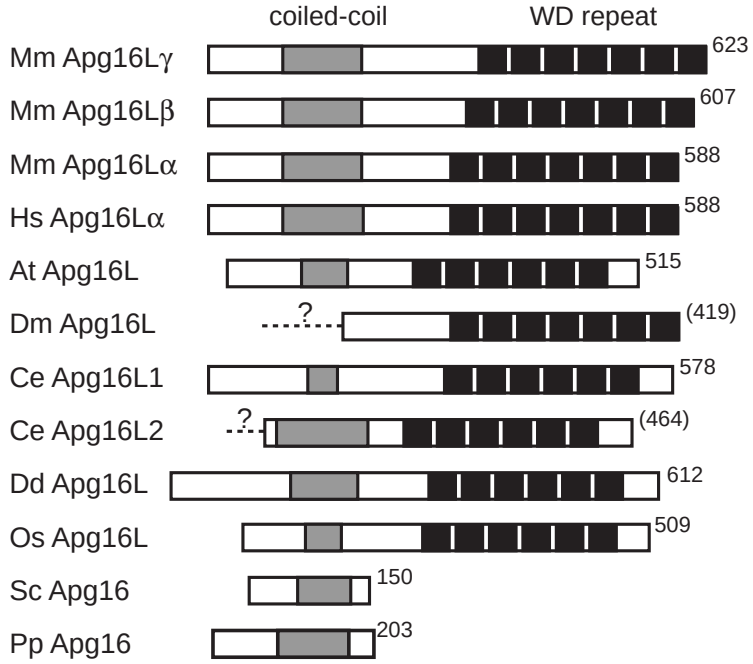

(b)

```
Mm Apg16L 106 LAQLVIDLNNQMQQKDKEIQMNEAKISEYLQTISDLETNC
                | : : |:|::    ::  | |   |   : :  |   |
Sc Apg16   28  LIRRLTDRNDKEAHLNELFQDNSGAIGGNIVSHDDALLNT

           146 L-----DLRTKLQDLEVANQT----------LKDEYDALQ
               |     :|::| |::    :           | ||  :
           68  LAILQKELKSKEQEIRRLKEVIALKNKNTERLNDELISGT

           171 ITFTALEEKLRKTTEENQELVTRWMAEKAQEANRLNAE
               | ||  ::||    :|: :|| ||: :  :|   :|:|
           108 IENNVLQQKLSDLKKEHSQLVARWLKKTEKETEAMNSE
```

Fig. 21 Putative homologues of Apg16L in other species. (a) Structural comparison of putative Apg16L homologues. The coiled-coil regions are indicated as grey boxes and the WD repeats are shown as black boxed. Mm, *Mus musculus*; Hs. *homo sapiens* (AK027854, AK024453; At, *Arabidopsis thalaiana* (AB024031); Dm,*Drosophila melanogaster* (AY058742); Ce, *Ceanorhabditis elegance* (U53340, U23449); Dd, *Dictyostelium descoideum* (AF019236); Os, *Oryza stiva* (AC087852); Sc, *Saccharomyces cerevisiae*; Pp, *Pichia pastoris* (Mukaiyama et al., 2002 and Y. Sakai, personal communication). The amino acid sequences of Dm Apg16L and Ce Apg16L, hypothesized from the genomic sequences, may be incomplete, lacking N-terminal sequences. (b) Amino acid sequence of mouse Apg16L was aligned with that of *S.cerevisiae* Apg16 using the BLAST2 program. Identical amino acids are shown with (|), while similar amino acids are indicated with (:).

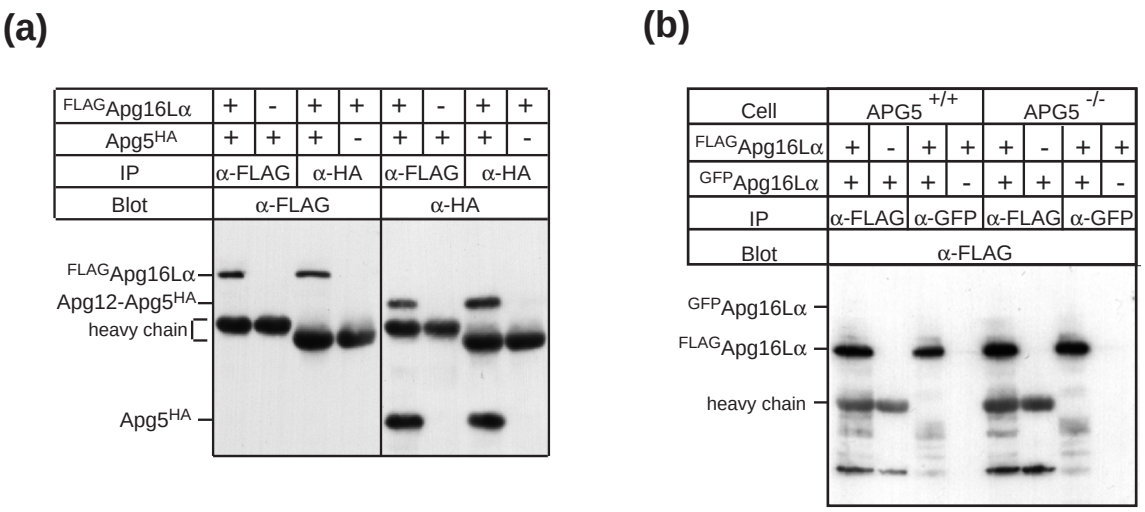

Fig. 22 Apg16L interacts with Apg5 and additonal Apg16L monomers. (a) FLAG-Apg16L and HA-Apg5 were immunoprecipitated from HeLa cells transiently transfected with the indicated plasmids. The interaction of these molcules was examined by western blot analysis using anti-FLAG and anti-HA antibodies. (b) Wild-type ES cells and Apg5$^{-/-}$ ES cells were transiently transfected with FLAG-Apg16L and/or GFP-Apg16L. Immunoprecipitates of GFP-APG16L were examined for the co-immunoprecipitation of FLAG-Apg16L by western blotting using anti-FLAG antibody.

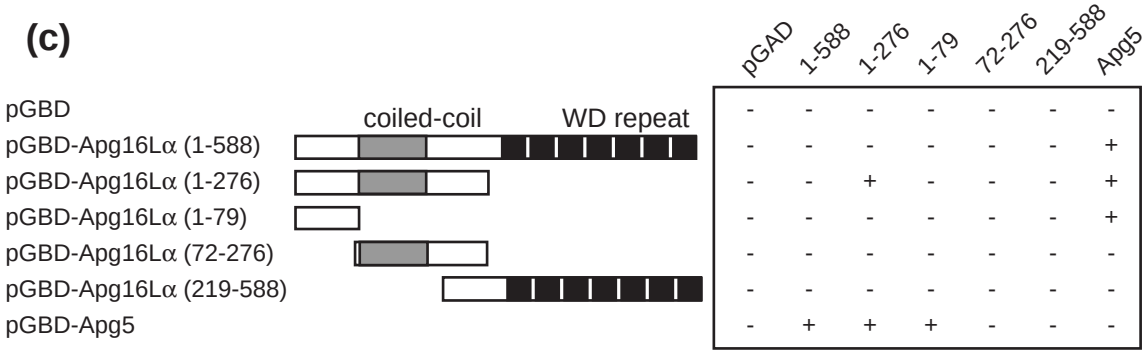

Fig. 23 Two-hybrid interactions of Apg16L-Apg5 and Apg16L-Apg16L.
Interactions between Apg16L, Apg16L deletion constructs and Apg5 within transfected yeast cells were assessed for growth on $His^{-}Trp^{-}Lue^{-}$ plate containg 3 mM 3-amino-triazole.

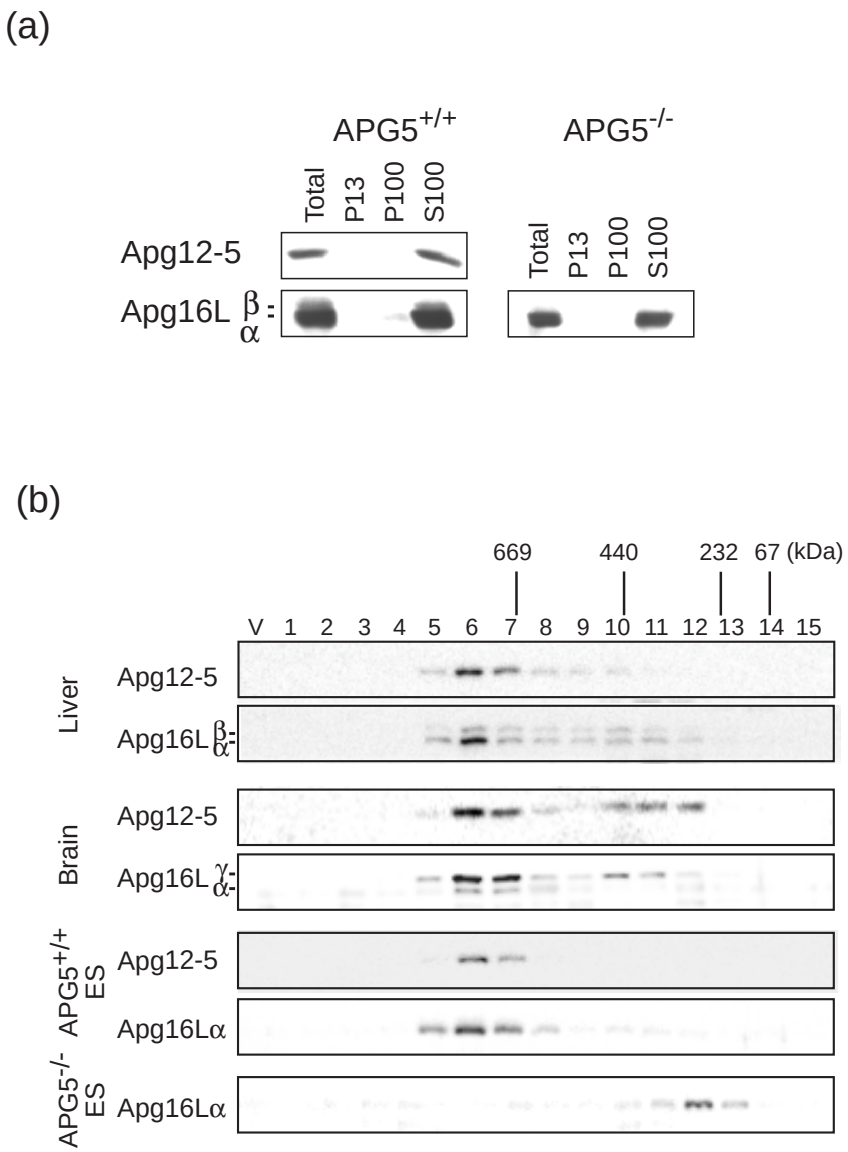

Fig. 24 Apg16L forms a ~800-kDa protein complex with Apg12-Apg5.
(a) Lysates from ES cells (Total) were fractionated into an initial pellet (P13) and a subsequencet pellet (P100) and suternatant (S100) fractions by differential centrifugateion. These fractions were analysed by immunoblotting using antibodies against Apg5 and Apg16L. (b) S100 fractions of tissue homogenates and cell lysates of wild-type and *APG5*$^{-/-}$ ES cells were separated by size exclusionchoromatography on a Superrose 6 column. Each fraction was subjected to immunoblotting using anti-Apg5 and anti-Apg16L antibodies. Positions of the molecular mass standards (in kDa) are shown. V, void fraction.

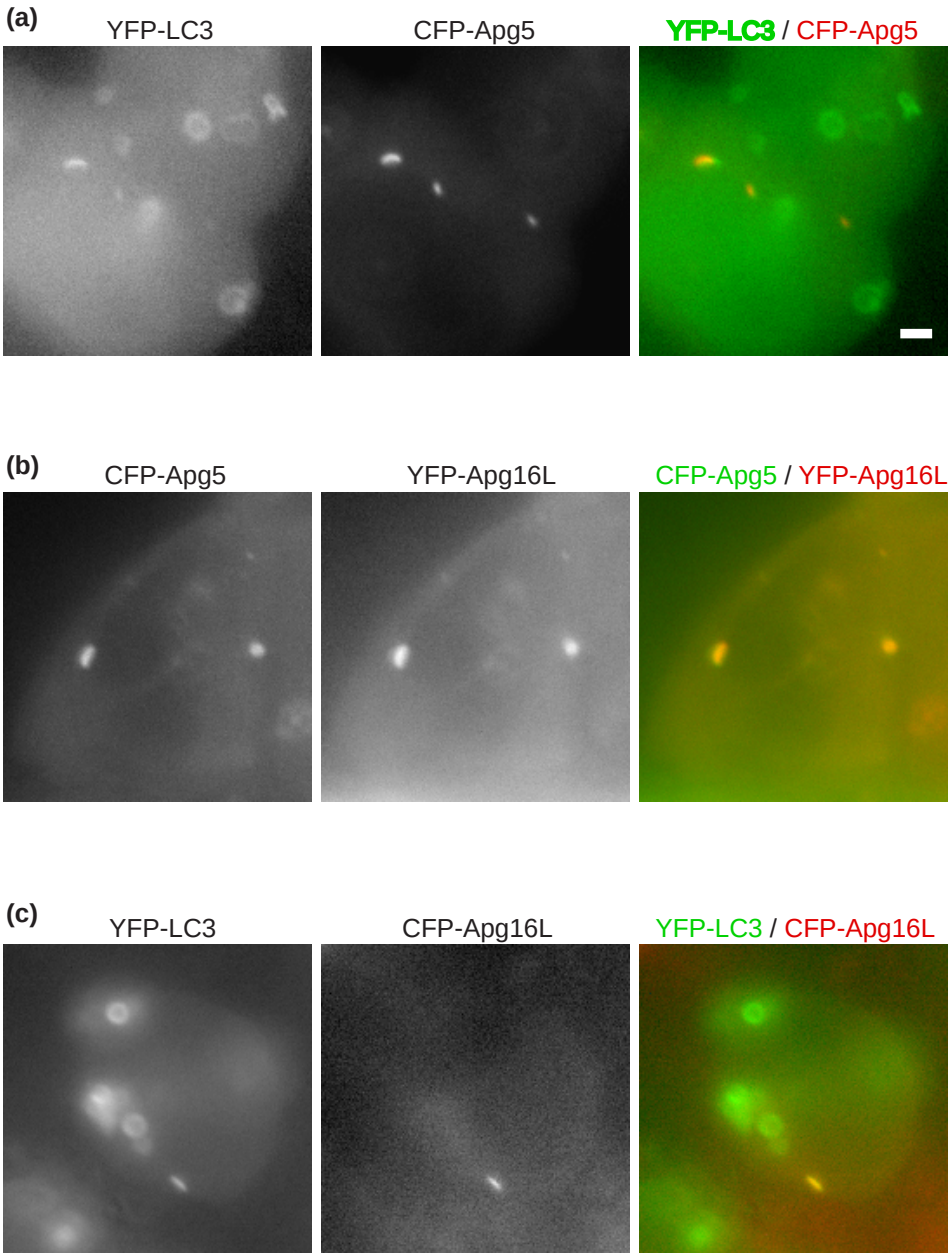

Fig. 25 Apg16L co-localizes completely with Apg5 and in part with LC3.
ES cells stably co-expressing (a) YFP-LC3 and CFP-Apg5 (clone F1-3), (b) CFP-Apg5 and YFP-Apg16L (clone Y63D-3), and (c) YFP-LC3 and CFP-Apg16L (clone B3-1-5) were cultured in Hanks' solution for 2 hours. Living cells were directly observed with a Delta Vision microscope system. Bar, 2μm.

Proteins	Function	Total clones
actinin-2	actin cross-linking	3
T6BP	apoptosis inhibition	1
PurB	initiating DNA reprication	1

1.3×10^7 transformants

Fig. 26 Two-hybrid screening of Apg16L-binding protein. A strain L40 carring pGBD-Apg16L was transformed with the library DNA (mouse embrionic cDNA library). Approximately 1.3×10^7 transformants were screened for the growth on SD plate media lacking Trp, Leu and His, but containg 1 mM 3-amino-1, 2, 4-triazole. From the positive clones obtaind with this screening, library plasmids were recovered and transfromed into L40 with pGBD-Apg16L again. The positive clones obtained 2nd screening, the nucleotide sequence of the insert DNA were determined.

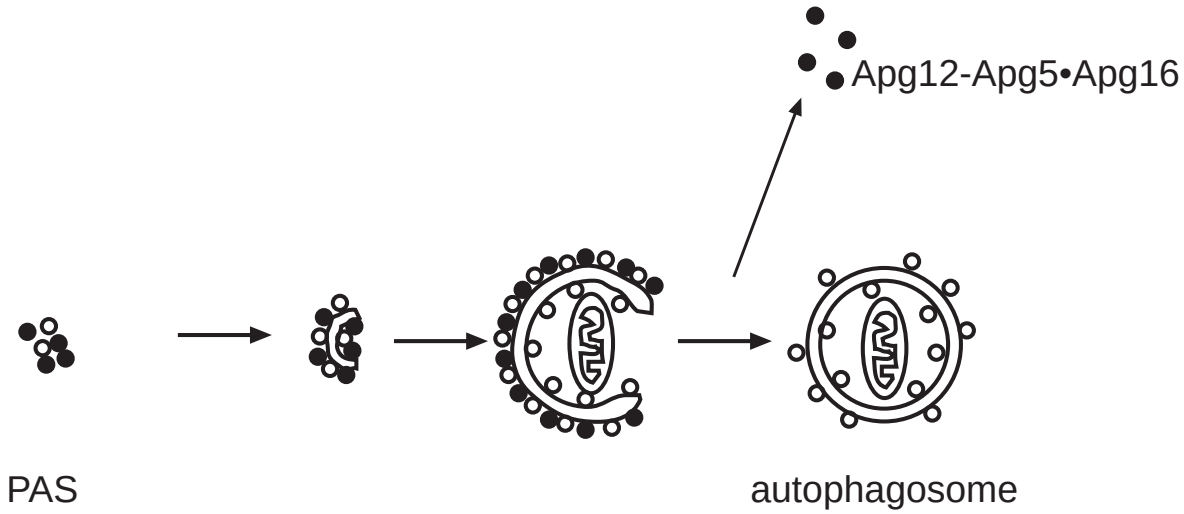

Fig. 27 The Apg12-Apg5*Apg16 complexes target from cytosol to PAS during autophagosome formation.

References

Ahlberg, J., and Glaumann, H. (1985). Uptake--microautophagy--and degradation of exogenous proteins by isolated rat liver lysosomes. Effects of pH, ATP, and inhibitors of proteolysis. Exp Mol Pathol *42*, 78-88.

Aplin, A., Jasionowski, T., Tuttle, D. L., Lenk, S. E., and Dunn, W. A., Jr. (1992). Cytoskel*et al* elements are required for the formation and maturation of autophagic vacuoles. J Cell Physiol *152*, 458-466.

Ashford, T.P., Porter, K.R. (1962). Cytoplasmic components in hepatic cell lysosome. J Cell Biol. 12, 198-202.

Baba, M., Takeshige, K., Baba, N., and Ohsumi, Y. (1994). Ultrastructural analysis of the autophagic process in yeast: Detection of autophagosomes and their characterization. J Cell Biol *124*, 903-913.

Baba, M., Osumi, M., and Ohsumi, Y. (1995). Analysis of the membrane structure involved in autophagy in yeast by freeze-replica method. Cell Struct Func *20*, 465-471.

Baba, M., Osumi, M., Scott, S. V., Klionsky, D. J., and Ohsumi, Y. (1997). Two distinct pathways for targeting proteins from the cytoplasm to the vacuole/lysosome. J Cell Biol *139*, 1687-1695.

Berggrun, A., and Sauer, R. T. (2001). Contributions of distinct quaternary contacts to cooperative operator binding by Mnt repressor. Proc Natl Acad Sci U S A *98*, 2301-2305.

Blommaart, E. F. C., Luiken, J. J. F. P., and Meijer, A. J. (1997). Autophagic proteolysis: control and specificity. Histochem J *29*, 365-385.

Cabezon, E., Butler, P. J., Runswick, M. J., and Walker, J. E. (2000). Modulation of the oligomerization state of the bovine F1-ATPase inhibitor protein, IF1, by pH. J Biol Chem *275*, 25460-25464.

Cuervo, A. M., and Dice, J. F. (1996). A receptor for the selective uptake and degradation of proteins by lysosomes. *273*, 501-503.

Cupers, P., Haar, E. T., Boll, W., and Kirchhausen, T. (1997). Parallel Dimers and Anti-parallel Tetramers Formed by Epidermal Growth Factor Receptor Pathway Substrate Clone 15 (EPS15). J Biol Chem *272*, 33430-33434.

Dawson, A. L., Beadle, D. J., Livingston, D. C., and Fisher, S. W. (1975). A histochemical study of acid phosphatase in normal and virus-transformed cultured fibroblasts. Histochem J *7*, 77-84.

De Duve, C. (1959). Lysosome, a new group of cytoplasmic particles, in Subcellular Particles. T. Hayashi, Editor. Ronald, New York, pp.128-159.

Dice, J. F. (1990). Peptide sequences that target cytosolic proteins for lysosomal proteolysis. Trends Biol Sci *15*, 305-309.

Dunn, W. A. (1994). Autophagy and related mechanisms of lysosome-mediated protein degradation. Trends Cell Biol *4*, 139-143.

George, M. D., Baba, M., Scott, S. V., Mizushima, N., Garrison, B. S., Ohsumi, Y., and Klionsky, D. J. (2000). Apg5p functions in the sequestration step in the cytoplasm-to-vacuole targeting and macroautophagy pathways. Mol Biol Cell *11*, 969-982.

Harding, T. M., Hefner-Gravink, A., Thumm, M., and Klionsky, D. J. (1996). Genetic and phenotypic overlap between autophagy and the cytoplasm to vacuole protein targeting pathway. J Biol Chem *271*, 17621-17624.

Hershko, A., and Ciechanover, A. (1998). The ubiquitin system. Annu Rev Biochem *67*, 425-479.

Hochstrasser, M. (1996). Ubiquitin-dependent protein degradation. Annu Rev Genet *30*, 405-439.

Hochstrasser, M. (2000). Evolution and function of ubiquitin-like protein-conjugation systems. Nat Cell Biol *2*, E153-E157.

Ichimura, Y., Kirisako, T., Takao, T., Satomi, Y., Shimonishi, Y., Ishihara, N., Mizushima, N., Tanida, I., Kominami, E., Ohsumi, M.*, et al.* (2000). A ubiquitin-like system mediates protein lipidation. Nature *408*, 488-492.

James, P., Halladay, J., and Craig, E. A. (1996). Genomic libraries and a host strain designed for highly efficient two-hybrid selection in yeast. Genetics *144*, 1425-1436.

Kabeya, Y., Mizushima, N., Ueno, T., Yamamoto, A., Kirisako, T., Noda, T., Kominami, E., Ohsumi, Y., and Yoshimori, T. (2000). LC3, a mammalian homologue of yeast Apg8p, is localized in autophagosome membranes after processing. EMBO J *19*, 5720-5728.

Kim, J., Dalton, V. M., Eggerton, K. P., Scott, S. V., and Klionsky, D. J. (1999). Apg7p/Cvt2p is required for the Cvt, macroautophagy, and peroxisome degradation pathway. Mol Biol Cell *10*, 1337-1351.

Kim, J., Huang, W. P., Stromhaug, P. E., and Klionsky, D. J. (2002). Convergence of multiple autophagy and cytoplasm to vacuole targeting components to a perivacuolar membrane compartment prior to de novo vesicle formation. J Biol Chem *277*, 763-773.

Kirisako, T., Baba, M., Ishihara, N., Miyazawa, K., Ohsumi, M., Yoshimori, T., Noda, T., and Ohsumi, Y. (1999). Formation process of autophagosome is traced with Apg8/Apg8p in yeast. J Cell Biol *147*, 435-446.

Kirisako, T., Ichimura, Y., Okada, H., Kabeya, Y., Mizushima, N., Yoshimori, T., Ohsumi, M., Takao, T., Noda, T., and Ohsumi, Y. (2000). The reversible modification regulates the membrane-binding state of Apg8/Apg8 essential for autophagy and the cytoplasm to vacuole targeting pathway. J Cell Biol *151*, 263-275.

Klionsky, D. J., Cueva, R., and Yaver, D. S. (1992). Aminopeptidase I of *Saccharomyces cerevisiae* is localized to the vacuole independent of the secretory pathway. J Cell Biol *119*, 287-299.

Komatsu, M., Tanida, I., Ueno, T., Ohsumi, M., Ohsumi, Y., and Kominami, E. (2001). The C-terminal region of an Apg7p/Cvt2p is required for homodimerization and is essential for its E1 activity and E1-E2 complex formation. J Biol Chem *276*, 9846-9854.

Lupas, A. (1996). Coiled-coils: new structures and new functions. Trends Biol Sci *21*, 375-382.

Mann, S. S., and Hammarback, J. A. (1994). Molecular characterization of light chain 3. J Biol Chem *269*, 11492-11497.

Michael F. K. and Thomas T. E. (2001) WD repeat domains target dictyostelium myosin heavy ahin kinases by binding directly to myosin filaments. J Biol Chem *276*, 6853.

Mizushima, N., Noda, T., and Ohsumi, Y. (1999). Apg16p is required for the function of the Apg12p-Apg5p conjugate in the yeast autophagy pathway. EMBO J *18*, 3888-3896.

Mizushima, N., Noda, T., Yoshimori, T., Tanaka, Y., Ishii, T., George, M. D., Klionsky, D. J., Ohsumi, M., and Ohsumi, Y. (1998a). A protein conjugation system essential for autophagy. Nature *395*, 395-398.

Mizushima, N., Sugita, H., Yoshimori, T., and Ohsumi, Y. (1998b). A new protein conjugation system in human. The counterpart of the yeast Apg12p conjugation system essential for autophagy. J Biol Chem *273*, 33889-33892.

Mizushima, N., Yamamoto, A., Hatano, M., Kobayashi, Y., Kabeya, Y., Suzuki, K., Tokuhisa, T., Ohsumi, Y., and Yoshimori, T. (2001). Dissection of autophagosome formation using Apg5-deficient mouse embryonic stem cells. J Cell Biol *152*, 657-667.

Mortimore, G. E., Lardeux, B. R., and Adams, C. E. (1988). Regulation of microautophagy and basal protein turnover in rat liver. Effects of short-term starvation. J Biol Chem *263*, 2506-2512.

Mortimore, G. E., and Poso, A. R. (1986). The lysosomal pathway of intracellular proteolysis in liver: regulation by amino acids. Adv Enzyme Regul *25*, 257-276.

Mortimore, G. E., Poso, A. R., and Lardeux, B. R. (1989). Mechanism and regulation of protein degradation in liver. Diabetes Metab Rev *5*, 49-70.

Natsume, T., Yamauchi, Y., Nakayama, H., Shinkawa, T., Yanagida, M., Takahashi, N., and Isobe, T. (2002). A direct nanoflow liquid chromatography-tandem mass spectrometry system for interaction proteomics. Anal Chem *74*, 4725-4733.

Noda, T., Matsuura, A., Wada, Y., and Ohsumi, Y. (1995). Novel system for monitoring autophagy in the yeast *Saccharomyces cerevisiae*. Biochem Biophys Res Commun *210*, 126-132.

Noda, T., and Ohsumi, Y. (1998). Tor, a phosphatidylinositol kinase homologue, controls autophagy in yeast. J Biol Chem *273*, 3963-3966.

Raught, B., Gingras, A.-C., and Sonenberg, N. (2001). The target of rapamycin (TOR) proteins. Proc Natl Acad Sci USA *98*, 7037-7044.

Sagiv, Y., Legesse-Miller, A., Porat, A., and Elazar, Z. (2000). GATE-16, a membrane transport modulator, interacts with NSF and the Golgi v-SNARE GOS-28. EMBO J *19*, 1494-1504.

Schmelzle, T., and Hall, M. N. (2000). Cell Tor, a central controller or cell growth. Cell *103*, 253-262.

Schworer, C. M., Shiffer, K. A., and Mortimore, G. E. (1981). Quantitative relationship between autophagy and proteolysis during graded amino acid deprivation in perfused rat liver. J Biol Chem *256*, 7652-7658.

Scott, S. V., Baba, M., Ohsumi, Y., and Klionsky, D. J. (1997). Aminopeptidase I is targeted to the vacuole by a nonclassical vesicular mechanism. J Cell Biol *138*, 37-44.

Scott, S. V., Hefner-Gravink, A., Morano, K. A., Noda, T., Ohsumi, Y., and Klionsky, D. J. (1996). Cytoplasm-to-vacuole targeting and autophagy employ the same machinery to deliver proteins to the yeast vacuole. Proc Natl Acad Sci U S A *93*, 12304-12308.

Shintani, T., Mizushima, N., Ogawa, Y., Matsuura, A., Noda, T., and Ohsumi, Y. (1999). Apg10p, a novel protein-conjugating enzyme essential for autophagy in yeast. EMBO J *18*, 5234-5241.

Smith, T. F., Gaitatzes, C., Saxena, K., and Neer, E. J. (1999). The WD repeat: a common architecture for diverse functions. Trends Biochem Sci *24*, 181-185.

Suzuki, K., Kirisako, T., Kamada, Y., Mizushima, N., Noda, T., and Ohsumi, Y. (2001). The pre-autophagosomal structure organized by concerted functions of APG genes is essential for autophagosome formation. EMBO J *20*, 5971-5981.

Takeshige, K., Baba, M., Tsuboi, S., Noda, T., and Ohsumi, Y. (1992). Autophagy in yeast demonstrated with proteinase-deficient mutants and conditions for its induction. J Cell Biol *119*, 301-311.

Tanida, I., Mizushima, N., Kiyooka, M., Ohsumi, M., Ueno, T., Ohsumi, Y., and Kominami, E. (1999). Apg7p/Cvt2p: a novel protein-activating enzyme essential for autophagy. Mol Biol Cell *10*, 1367-1379.

Terlecky, S. R., Chiang, H. L., Olson, T. S., and Dice, J. F. (1992). Protein and peptide binding and stimulation of in vitro lysosomal proteolysis by the 73-kDa heat shock cognate protein. J Biol Chem *267*, 9202-9209.

Thumm, M., Egner, R., Koch, B., Schlumpberger, M., Straub, M., Veenhuis, M., and Wolf, D. H. (1994). Isolation of autophagocytosis mutants of *Saccharomyces cerevisiae*. FEBS Lett *349*, 275-280.

Tsukada, M., and Ohsumi, Y. (1993). Isolation and characterization of autophagy-defective mutants of *Saccharomyces cerevisiae*. FEBS Lett *333*, 169-174.

Wang, H., Bedford, F. K., Brandon, N. J., Moss, S. J., and Olsen, R. W. (1999). $GABA_A$-receptor-associated protein links GAB_A receptors and the cytoskeleton. Nature *397*, 69-72.

Yoshimori, T., Yamagata, F., Yamamoto, A., Mizushima, N., Kabeya, Y., Nara, A., Miwako, I., Ohashi, M., Ohsumi, M., and Ohsumi, Y. (2000). The mouse SKD1, a homologue of yeast Vps4p, is required for normal endosomal trafficking and morphology in mammalian cells. Mol Biol Cell *11*, 747-763.

Yuan, W., Stromhaug, P. E., and Dunn Jr, W. A. (1999). Glucose-induced microautophagy of peroxysomes in *Pichia pastoris* requires a unique E1-like protein. Mol Biol Cell *10*, 1353-1366.